University of Maribor

Faculty of Energy Technology

Journal of ENERGY TECHNOLOGY

Volume 15 / Issue 3

NOVEMBER 2022

www.fe.um.si/jet.html

Journal of ENERGY TECHNOLOGY

VOLUME 15 / Issue 3

Revija Journal of Energy Technology (JET) je indeksirana v bazah INSPEC© in Proquest's Technology Research Database.

The Journal of Energy Technology (JET) is indexed and abstracted in database INSPEC© and Proquest's Technology Research Database.

JOURNAL OF ENERGY TECHNOLOGY

Ustanovitelj / FOUNDER

Fakulteta za energetiko, UNIVERZA V MARIBORU /
FACULTY OF ENERGY TECHNOLOGY, UNIVERSITY OF MARIBOR

Izdajatelj / PUBLISHER

Fakulteta za energetiko, UNIVERZA V MARIBORU /
FACULTY OF ENERGY TECHNOLOGY, UNIVERSITY OF MARIBOR

Tehnični urednik / TECHNICAL EDITOR

Sonja Novak

Tehnična podpora / TECHNICAL SUPPORT

Tamara BREČKO BOGOVČIČ

Izhajanje revije / PUBLISHING

Revija izhaja štirikrat letno v nakladi 100 izvodov. Članki so dostopni na spletni strani revije – https://www.fe.um.si/jet.html / The journal is published four times a year. Articles are available at the journal's home page – www.fe.um.si/en/jet.html.

Cena posameznega izvoda revije (brez DDV) / Price per issue (VAT not included in price): 50,00 EUR

Informacije o naročninah: https://www.fe.um.si/naro%C4%8Dnine.html / Subscription information: https://www.fe.um.si/en/subscriptions.html

Lektoriranje / LANGUAGE EDITING

TAIA INT d.o.o.

Oblikovanje in tisk / DESIGN AND PRINT

Tiskarna Koštomaj d.o.o.

Naslovna fotografija / COVER PHOTOGRAPH

Jurij AVSEC

Oblikovanje znaka revije / JOURNAL AND LOGO DESIGN

Andrej PREDIN

Ustanovni urednik / FOUNDING EDITOR

Andrej PREDIN

Izdajanje revije JET finančno podpira Javna agencija za raziskovalno dejavnost Republike Slovenije iz sredstev državnega proračuna iz naslova razpisa za sofinanciranje domačih znanstvenih periodičnih publikacij / The Journal of Energy Technology is co-financed by the Slovenian Research Agency.

Spoštovani bralci revije Journal of energy technology (JET)

Energetska situacija v Sloveniji, kot tudi po Evropi, je izredno negotova. Kadar govorimo o energiji, mislimo na električno energijo, potrebo po toplotni in hladilni energiji ter na energijo goriva, ki je potrebna za transport. Zaradi vojne v Ukrajini in nekaterih drugih dejavnikov cene energije globalno naraščajo, napovedi za bližnjo prihodnost pa so posledično negotove in nepredvidljive. V luči trenutnih okoliščin in energetskih obvez Slovenije smo tudi pri nas začeli pospešeno iskati alternativne vire energije – pridobivanje vodika iz vode in biomase ter pridobivanje določenih biogoriv iz biomase. Tako stara celina kot ves svet sta v zadnjem času prizorišče drastičnih sprememb: poleg vodikovih polnilnih postaj se v Evropi predvideva gradnja novih oz. razširitev že obstoječih vodikovodov. Hkrati smo priča intenzivnemu razvoju avtomobilov, vlakov, ladij, letal in drugih prevoznih sredstev na vodik. Želimo si, da se bomo tudi v Sloveniji odločili za razvoj dela industrije v tej smeri, saj se v bližnji prihodnosti na tem področju in na področju izrabe obnovljivih virov obetajo velike investicije v razvoj.

Jurij AVSEC
odgovorni urednik revije JET

Dear Readers of the Journal of Energy Technology (JET)

The energy situation in Slovenia, and across Europe in fact, is very uncertain. When we talk about energy, we mean electricity and the need for thermal energy and cooling energy, as well the energy produced by fuels for transport. Due to the war in Ukraine and numerous other factors, energy prices are rising globally, and projections for the near future are very uncertain and unpredictable. Due to this situation, and owing to Slovenia's energy obligations, the possibility of obtaining hydrogen from water and biomass and obtaining some other biofuels from biomass has arisen. Both in Europe and across the world, drastic changes have been taking place recently; besides hydrogen filling stations, the construction or expansion of already existing hydrogen pipelines is foreseen in Europe. Efforts towards the development of new hydrogen-powered cars, trains, ships, planes and other means of transport have also been very intensive. We can only hope that Slovenia will also develop part of the industry in this direction, as large investments in development are expected in the near future, not just in this area but in the area of renewable resources as a whole.

Jurij AVSEC
Editor-in-chief of JET

Table of Contents / Kazalo

Journal of Energy Technology

JET Volume 15 (2022) p.p. 11-24
Issue 3, 2022
Type of article: 1.01
www.fe.um.si/si/jet.html

THE USE OF DIFFERENTIAL EVOLUTION TO DETERMINE MAXIMUM GENERATION AND LOAD VALUES IN THE DISTRIBUTION NETWORK

UPORABA DIFERENČNE EVOLUCIJE ZA DOLOČITEV NAJVEČJE PROIZVODNJE TER PORABE V DISTRIBUCIJSKEM OMREŽJU

Eva Tratnik[ℜ1], Janez Ribič[1], Matej Pintarič[1], Miran Rošer[2], Gorazd Štumberger[1], Miloš Beković[1]

Keywords: distribution network, renewable energy sources, optimisation method, voltage profile

Abstract

By integrating renewable energy sources into the existing distribution network, the characteristics and local stability of the network is highly impacted. The network, which was built with the goal of a directed energy flow from large conventional sources connected to the transmission network via the distribution network to consumers, can change the direction of the energy flow. The adoption of environmental commitments and directives encourages the integration of local dispersed energy sources, which can worsen voltage conditions in the distribution network. To avoid excessive local production, distribution network operators must limit the installation of

[ℜ] Corresponding author: Eva Tratnik, Tel.: +386 (0)2-220-7086, University of Maribor, Faculty of Electrical Engineering and Computer Science, Koroška cesta 46, 2000 Maribor, Slovenia, E-mail address: eva.tratnik@um.si

[1] University of Maribor, Faculty of Electrical Engineering and Computer Science, Koroška cesta 46, 2000 Maribor, Slovenia

[2] Elektro Celje d.d., Vrunčeva ulica 2a, 3000 Celje

new generation units, as it is necessary to take into account the quality of power supply by monitoring its network parameters, such as the appropriate voltage profile and the ratio between active and reactive power. On the other hand, excessive loads due to the mass transition of household heating and transport towards electricity can also pose a problem for high-quality electricity supply due to the excessive voltage drop. The article presents an algorithm for determining the maximum size of unit production and the maximum load at a node in the distribution network. Also demonstrated is the use of variable tap transformer technology, which adjusts the tap of the transformer to provide an appropriate voltage profile in the network. The entire analysis was performed on a model of a real medium-voltage network, in which solar and hydropower plants are already included. The model was verified by comparing its calculated values with actual measurements. The goal was to determine the size of the unit's maximum production, as well as the size of the maximum load, by using the differential evolution algorithm, while keeping voltage profiles within the permissible limits. The results of the analysis are presented in the article.

Povzetek

Z vključevanjem obnovljivih virov energije v obstoječe distribucijsko omrežje vplivamo na karakteristike in lokalno stabilnost omrežja. Omrežje, ki je bilo zgrajeno s ciljem usmerjenega pretoka energije od velikih konvencionalnih virov, priklopljenih na prenosno omrežje preko distribucijskega omrežja do porabnikov, lahko spreminja usmerjenost pretoka energije. Sprejetje okoljskih zavez in direktiv spodbuja integracijo lokalnih razpršenih virov energije, ki lahko poslabša napetostne razmere v distribucijskem omrežju. V izogib čezmerni lokalni proizvodnji želijo operaterji distribucijskih omrežij omejiti priklapljanje novih proizvodnih enot, saj je treba upoštevati kakovostno oskrbo s spremljanjem parametrov omrežja, kot sta ustrezen napetostni profil ter razmerje med delovno in jalovo močjo. Prevelika bremena pa zaradi množičnega prehoda ogrevanja in transporta na električno energijo prav tako prestavljajo težavo za kakovostno oskrbo z električno energijo. V članku je predstavljen algoritem za določitev največje velikosti proizvodnje enote in največjega bremena v vozlišču v distribucijskem omrežju. Prikazana je tudi uporaba tehnologije transformatorja s spremenljivo prestavo, ki prilagodi prestavo transformatorja tako, da zagotovi ustrezen napetostni profil v omrežju. Celotna analiza je bila narejena na modelu realnega srednjenapetostnega omrežja, v katerega so že vključene sončne in hidroelektrarne. Model je bil verificiran tako, da smo izračunane vrednosti modela primerjali z dejanskimi meritvami. Cilj je določiti velikosti maksimalne proizvodnje enote in bremena z uporabo algoritma diferenčne evolucije, pri tem pa ohraniti napetostne razmere znotraj dopustnih meja. V članku so predstavljeni rezultati opravljene analize.

1 INTRODUCTION

With the development of dispersed sources of production and environmental protection commitments, the distribution network has undergone a major transformation in recent years. If in the past it was considered a passive part of the power grid with a consumer character, with the integration of distributed sources it is turning into an active one. As a result of the change in network activity, new requirements for network operation and the need for advanced planning algorithms and optimisation of network operation arise. To analyse operating conditions and energy flows in the network, it was necessary to develop appropriate models that describe conditions in the network. These algorithms need to be adapted, since distribution networks are mostly radial in nature, while transmission networks are closed-looped. By including distributed sources and larger loads in the distribution network, the voltage profiles are heavily influenced. The main problem with distributed sources of electricity is that the production of electricity depends on meteorological conditions and/or the time of day. Due to unreliable and unpredictable current production from scattered sources, it is difficult to coordinate current consumption. Therefore, local power surges may occur in the network, where voltages in the lines may exceed the permissible values in the case of excessive production, and at the same time voltages may drop sharply below the permissible value in the case of excessive loads. Adequate voltage conditions can be ensured by several methods and measures, such as: changing the topology of the network or even by replacing conductors with ones of larger cross-sections. These measures are passive, usually very expensive and sometimes not the most optimal; sometimes the optimal placement of distributed resources in the network is sufficient.

Chapter 2 presents the creation of the network model and verification; Chapter 3 presents the results of the analysis. The analysis is divided into several parts: the first part consists of the analysis of the current situation in the network, the second part consists of the analysis of determining the maximum production and the maximum load for a summer and winter day, and the third part consists of the introduction of OLTC, when we include production units in the network that cause an increase in voltage in a network that is larger than allowed. Chapter 4 presents the conclusion.

2 DESCRIPTION OF METHODS AND MODEL VERIFICATION

The article discusses a practical example of the operation of a radial medium-voltage distribution line. Data about the network topology and the parameters of the network elements were obtained from the distribution company. The data was processed as shown in Figure 1, where the original *shp* data is converted to *Excel* using the *Qgis* program and imported into the *Matlab* environment, where all further network analysis and later optimisations are carried out.

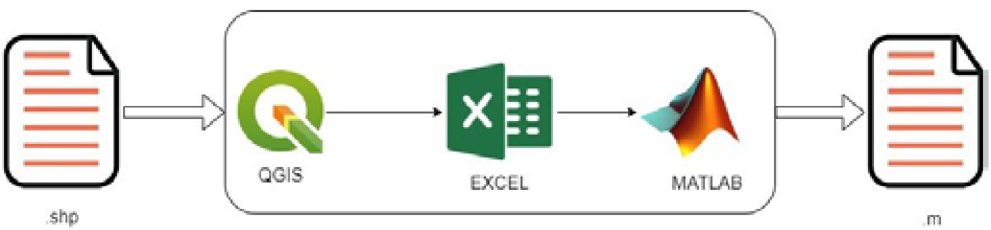

***Figure 1**: Conversion of data from the distribution operator into a structure for resolving electrical networks*

To create the network model, a *Matlab* environment was used, where a network model for the calculation of voltage conditions for the planned topology and parameters of the lines was created. The model of the considered network with thirty-six nodes is shown symbolically in Figure 2, where nodes in which solar or hydro power plants already connected are marked in red. For the purposes of the analysis, any node could be changed arbitrarily.

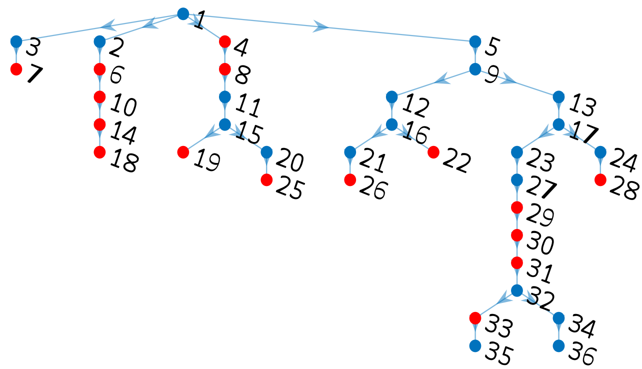

Figure 2: *Renumbered topology of considered radial distribution network*

The three solar power plants (PV) and five hydroelectric power plants (HPP) are included in the network. Data on the nominal generated power P_{gen} and the type of individual production of the unit are shown in Table 1.

Table 1: *Rated power and type of power plant included in the specific node*

	Node	P_{gen} [kW]	Type
TP 1	30	22	PV
TP 2	31	0	/
TP 3	14	276	HPP
TP 4	35	11	PV
TP 5	10	169	HPP
TP 6	26	1316	HPP
TP 7	18	287	HPP
TP 8	7	0	/
TP 9	4	160	HPP
TP 10	8	0	/
TP 11	25	207	HPP
TP 12	6	49	PV
TP 13	19	205	HPP
TP 14	29	0	/
TP 15	22	0	/
TP 16	28	0	/

The created network model, which has been built, was also verified before further analysis. Several types of load flow methods are known [2,3,5], but in this case the BFS algorithm has been used [1]. Verification of the calculation was carried out by calculating on an arbitrary day and at any measurement point, where the two years of measurement data were available with ninety-six measurement samples per day at 15-minute time intervals, therefore giving over 70,000 measurement points in total. The goal of verification is to check the accuracy of the calculation of the built model by comparing the results with measurements.

In Figure 3, a comparison for the selected day is presented, where a comparison between the measured voltage value and the calculated voltage values in each phase can be seen. A minor asymmetry is visible in phase *L*1, whilst in phases *L*2 and *L*3 correspondence with the measurements is satisfactory. Based on many selected currents and several days, we can conclude that the built model realistically describes the voltage situation and that it can be used for the study of potential new loads as well as new dispersed sources.

In Figure 3, on the left, it can be seen that the same *P* and *Q* values as were used for the measurements were used for the model calculation. The graph on the right shows the voltages, where it can be seen that in the case of phases *L*1 and *L2* there is a relatively good match, while in phase *L*3 there is a smaller deviation, but this model cannot take this into account.

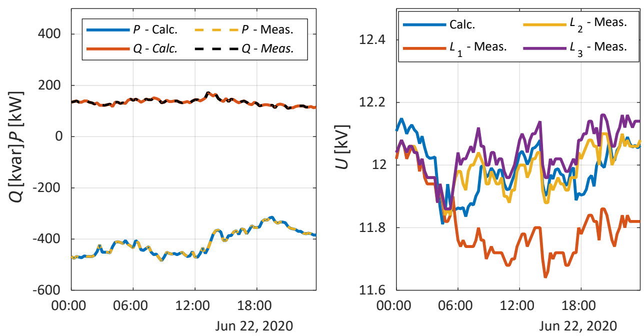

Figure 3: *Comparison of calculations and measurements for selected day*

After the verification of the model, the next step was to utilise an optimisation, which is a process of finding the parameters of the function so that the final value of the function cannot be improved. This means that, using optimisation methods, the optimum that gives either the lowest or the highest function value was found. Several types of optimisation methods are known [4,6,7], but in this case the differential evolution algorithm has been used. The differential evolution flow chart is shown in Figure 4. The optimisation process starts with the generation of NP randomly selected vectors of dimension *D*. Then the following operations are performed: mutation, crossover and selection [8].

The optimisation seeks the minimum of the criterion function, which is defined as (2.1) in the case where only one parameter is sought:

$$q = \frac{1}{x_p(1)} + p \tag{2.1}$$

When two parameters are sought, the criterion function is written by (2.2), and similarly the optimisation can be extended to more parameters.

$$q = \left(\frac{1}{x_p(1)} + \frac{1}{x_p(2)}\right) + p \tag{2.2}$$

In the context of the discussed issue of adding production units or additional loads, let's say that in the first case we were only looking for a single-criteria optimisation using equation (1), and in the case of a dual-criteria optimisation using equation (2) we were simultaneously looking for P_L and P_G in different nodes. In both equations, the variable p represents penalties or penalty functions, which are designed in such a way that by including additional production or load, we do not exceed the voltage limits.

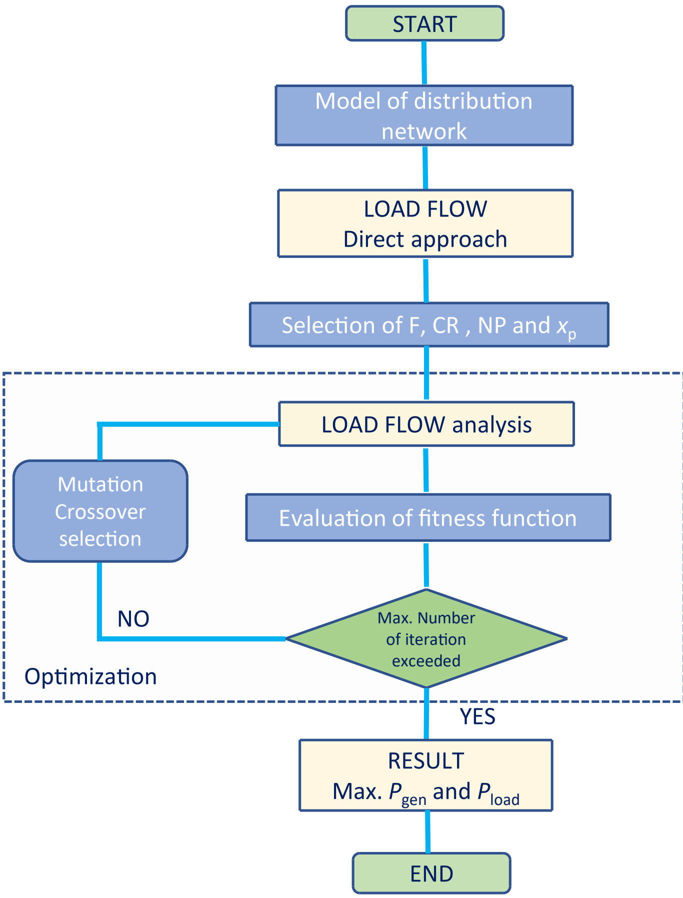

Figure 4: *Flowchart of the proposed procedure for the optimisation of network operation*

Voltage quality problems can occur in the network, meaning the voltage in the network is too low or too high. The permissible limits between which the voltage can fluctuate are prescribed in the SIST EN 50160 standard and are usually ±10%. There are several ways to solve the problems of too low or too high voltages. One possibility is to replace long-distance cable connections of smaller cross-sections with cables of larger cross-sections, change the network topology, and other such changes. Although these solutions are technically easy to implement and bring an additional benefit in terms of reduced electricity losses, they have a high investment cost. In the distribution network, voltage regulation is also possible using OLTC (On Load Tap Changer). A medium voltage/low voltage transformer with OLTC can have 9 taps and is able to regulate the voltage in steps of ±3%. The selected transformer can decrease or increase the voltage by a maximum of 12% of the nominal voltage [9].

3 RESULTS

On the built and verified model, the maximum network limits for adding new elements to any node of the network can be checked on the real network parameters.

3.1 Analysis of the current situation in the network

Figure 5 shows the analysis of non-zero load nodes. Six such nodes exist with a unique loading profile, with the largest load being in node 27. A similar analysis is also done for the production units for the selected day in January, where out of every thirty-five nodes, only seven are generating energy, the others being negligible. Figure 6 shows that some production units are independent of the time of day, considered as production from small hydropower plants, while production from solar power plants depends on the time of day.

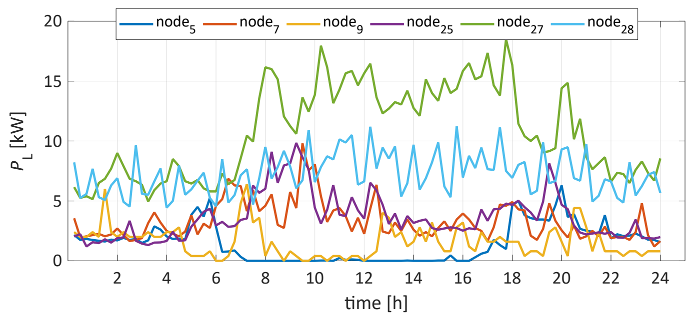

Figure 5: *Loading profile of selected nodes for a winter day, January 5th*

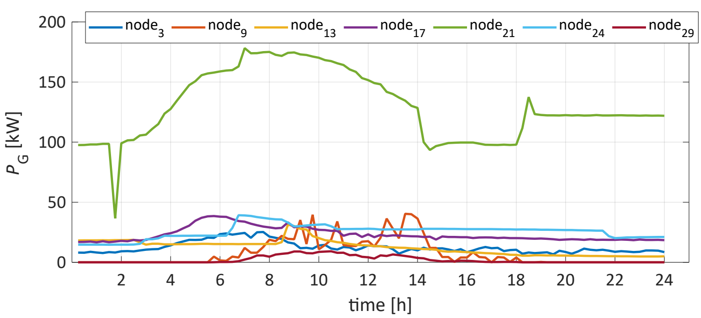

Figure 6: *Generation profile of selected nodes for a winter day, January 5th*

The analysis of voltage conditions does not change significantly over a single day in all 15-minute intervals, so the results for a working day of the year are presented for a selected part of the day, because the values deviate the most from the average profile. Figure 7 shows an analysis of the voltage profiles at an individual node, where either the minimum values or the maximum values for the month are presented. The highest voltage occurs in the month of February, while the lowest occurs in September. From this it can be concluded that for all 365 days and all ninety-six 15-minute interval measured values each day, only those of potential concern are plotted. Based on permissible voltage limits, it can be concluded that there are no problems with the voltage profile in the considered network. On the other hand, the effects of additional elements in the network can be analysed and their maximum values can be estimated so that the values are still within the prescribed limits.

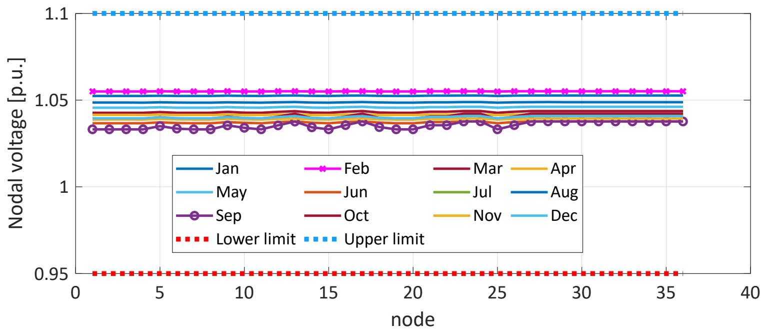

Figure 7: *Voltage profile throughout the year for a worst case scenario*

3.2 Determination of maximum load and maximum production unit

On the left in Figure 8, the voltage distribution when additional production units are added to the selected node 9 is shown. For the selected day and the selected moment of the day, a relatively large generating unit can be added to the node and at the same time the voltage profile is kept within the permissible limits of +10%. When the limit is exceeded, as in the case of +50 MW, the voltage in a larger number of nodes is exceeded, and nodes are immune to addition depending on the network topology. A similar analysis is made for adding loads to the node, as shown on the right in Figure 8. More than 80 MW of load can be added to node 9 without worsening the voltage profile, but in the case of 100 MW the values exceed the permissible limits.

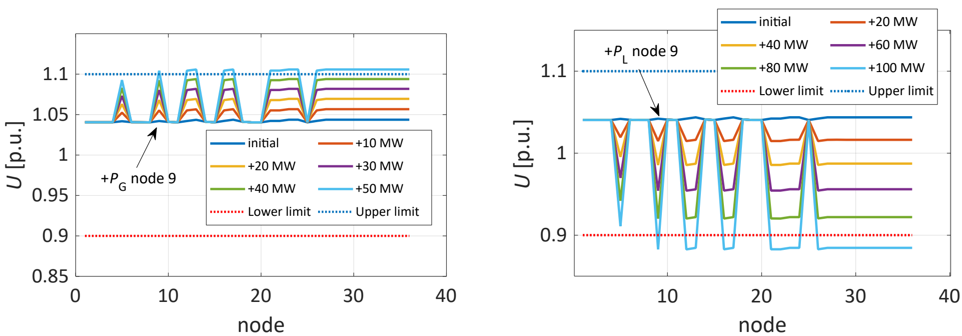

Figure 8: *Voltage profile in all thirty-five nodes while adding generation unit into node 9 (left) and adding load (right)*

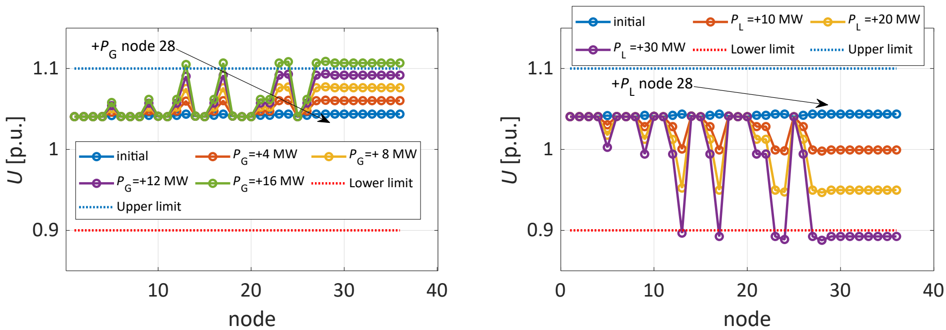

Figure 9: *Voltage profile in all thirty-five nodes while adding generation unit into node 28 (left) and adding load (right)*

A similar analysis can be performed for any node, as presented for the example of node 28 in Figure 9. The graph on the left shows that adding generating units again raises the voltage, and the limit is exceeded for the added 16 MW. It can also be observed that when adding loads, the voltage decreases, as shown in the graph on the right, where the limit is exceeded at an added load of 30 MW. In the rest of the article, the simultaneous addition of loads and generators is presented, but before that, an annual analysis of the situation in the network is presented.

As presented so far, changes to both loads and production are conducted manually, and only for the selected moment of the selected day. If the goal is to give a definitive answer about the maximum values of additional elements, it is necessary to perform a substantial number of calculations. It is simpler to use the optimisation algorithm from Figure 4, where calculations can be performed arbitrarily for each non-balance node.

On the left in Figure 10, the calculation of the maximum unit production for nodes 2 to 36 for both summer and winter days is shown. On the right-hand side, the calculation of the maximum load for nodes is shown. The calculation of the maximum production or load is calculated so that the voltage remains within the permissible limits. Since the network is radial, larger unit productions can be included at the beginning of the lines, and the closer we get to the nodes at the end of the lines, the smaller the calculated maximum unit production size is. The optimisation process is similar to the graphs in Figures 8 and 9, except that in a maximum of 50 iterations the result converges to the satisfactory value.

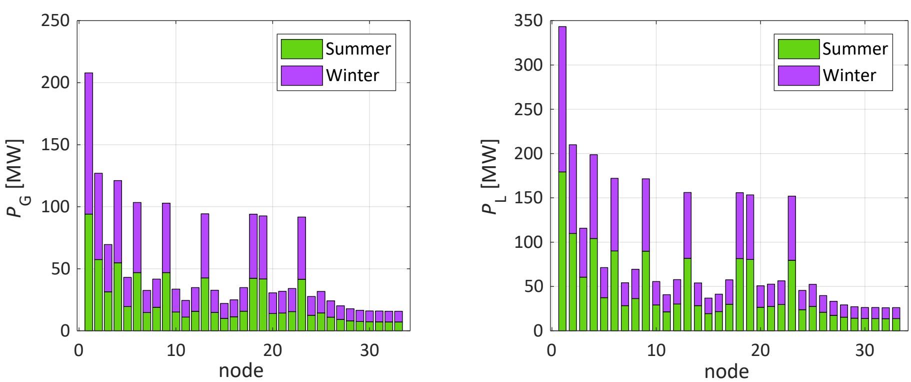

Figure 10: *Values of P_G and P_L for nodes 2 to 36 over two seasons*

However, we can conclude that the values calculated in the latter analysis are not necessarily final if the described OLTC device is installed in the network. The continuation presents an analysis of what can happen in the network when a production unit is connected to the network, which, due to its operation, causes the voltage to rise above the permitted limit. As many as two production units in nodes 21 and 22 are included in the network. Figure 11 displays the topography of the network, on which the location of the OLTC is visible (node 16, in red) and the nodes in which additional production units are added are marked with P_{gen}, node 21 and 22.

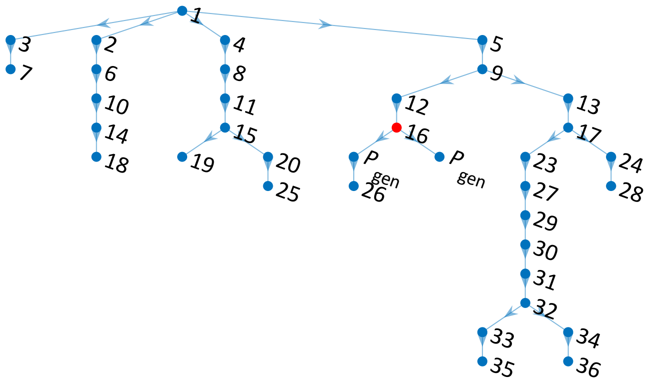

Figure 11: *Topology of considered radial distribution network with marked node with OLTC and nodes of additional generation units*

Figure 12a shows the additional production unit for node 21 over time. A 20 MW generating unit is connected to the grid, which operates at a constant power throughout the day, and at 11:00 a 20 MW generating unit is added to it. Figure 12b shows the same for node 22, except that the additional generating unit is connected later.

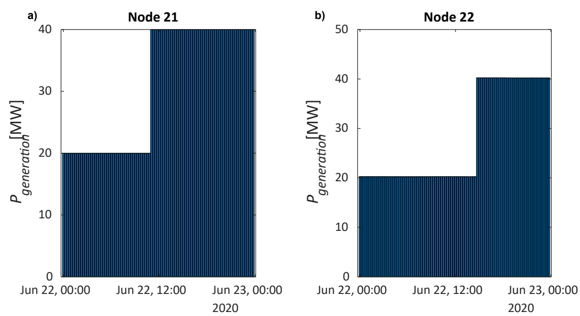

Figure 12: *Change adding production unit to two nodes after OLTC operation*

Figure 13a presents the voltage conditions before and after the operation of the OLTC. The voltage before the activation of the OLTC has already exceeded the permissible limits, and since we turn on the additional generation in nodes 21 and 22 at 00:00, the OLTC level changes at the first moment of the day. This lowers the voltage so that it is within acceptable limits. Then, the OLTC rate remains the same, even though we include an additional 20 MW generating unit in node 21 at 11:00. The OLTC rate increases only when an additional generating unit is connected to the grid at node 22 at 14:45, as shown in Figure 13b.

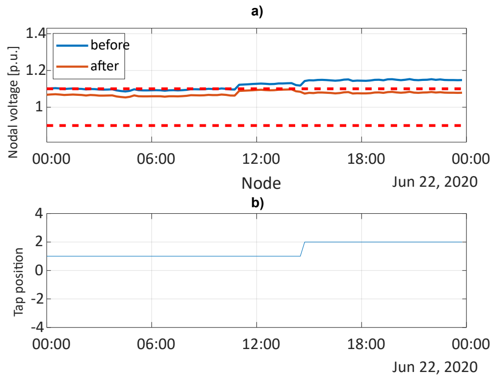

Figure 13: *Voltage before and after the application of the OLTC and display of the degree of OLTC taps for the selected case over time*

From the latter analysis, it is clear that optimisation algorithms can be used to check the network's limitations, which, however, are not final, but can also be changed by adding dynamic elements such as OLTC.

3.3 Simultaneous addition of load and production units

A particularly interesting analysis is the simultaneous addition of load and production units to different nodes, where one raises and the other lowers the voltage in the node. It is also necessary to realise that there are as many as ninety-six different moments in time available for all 365 days of the year, which, with all the possible combinations of the thirty-five nodes, results in an complex multitude of variants. Figure 14 shows two examples where both combinations on the two selected nodes, 9 and 28, were made, as in the analysis above. In the graph on the left, node 9 is the additional production unit and node 28 is the additional load, while the graph on the right it is the opposite. In the example on the left, calculation started at the previous limits, i.e. in node 9 P_G = +40 MW and P_L = +30 MW, it is noticeable that in the case of the simultaneous addition of both elements, the limit power of both units changes disproportionately, namely the maximum production in node 9 changes to a value of 105 MW and the maximum load in node 28 to 50 MW.

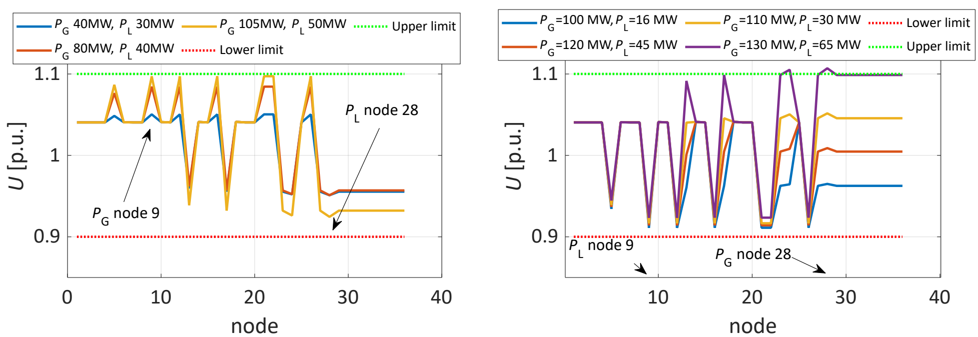

Figure 14: *Voltage profile in all thirty-five nodes while adding a generation unit into node 28 (left) and adding load (right)*

The graph on the right shows the opposite, as this time node 9 has a load imposed and node 28 a unit of production. The analysis shows that the previous limit values, such as for the case of independent analyses, namely $P_{G\text{-}28node}$ = 100 MW and $P_{L\text{-}9node}$ = 15 MW, do not cause problems. When both values are increased, they tentatively stop at 130 MW for node 28, and 65 MW for node 9.

Such a manual analysis is not suitable, since the changes are contradictory and non-linear, so the use of optimisation algorithms makes sense. In addition, an exact value of the limits is also achieved, which can be changed at will, but in this case they are set to ±10%.

The result of employing the optimisation algorithm to the problems mentioned are displayed in Figure 15. The graph on the left shows the voltage distribution for all nodes where the two target nodes for adding additional units are selected; a production unit is added to node 35, while a load is added to node 25. In the graph on the left, only one in five of the thirty-five optimisation iterations are shown, so that it is easy to see how, when adding the two additional elements, the voltage values increasingly converge towards the limit values. This means that when adding loads, the voltages at certain nodes approach the lower limit of 90% of the nominal value (nodes 8, 11, 15, 19 and 20), and when adding an additional generating unit to node 35, only at this node the voltage rises to the extreme values of 110% of the nominal value. The graph in the upper right shows how the search values change, and the graph below shows the convergence of the optimisation algorithm. It can be seen that the chosen number of iterations is thirty-five, and it proves to be sufficient, as the estimated error is less than 1% and the results are also satisfactory. Depending on the selected location of additional elements in the network, a production unit in node 35, size $P_{G\text{-}35}$ = 28.68 MW, and an additional load in node 25, size $P_{L\text{-}25}$ = 7.17 MW, can be connected to the network for the selected day and time.

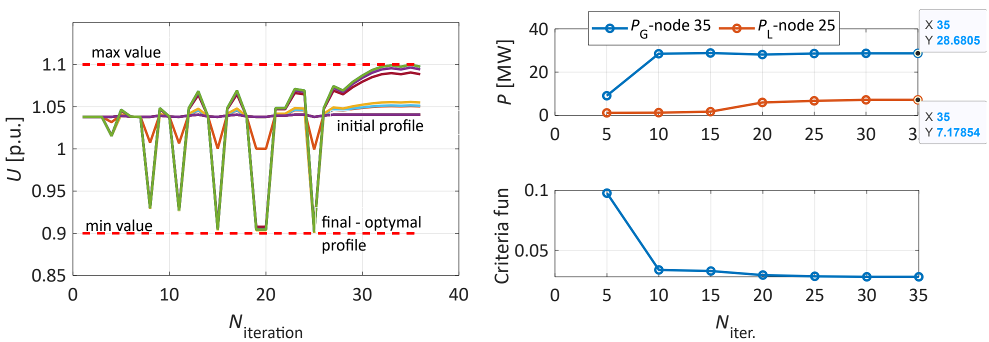

Figure 15: *Voltage profile in all thirty-five nodes while adding a generation unit into node 35 (left) and adding load to node 25, optimisation evolution on the right*

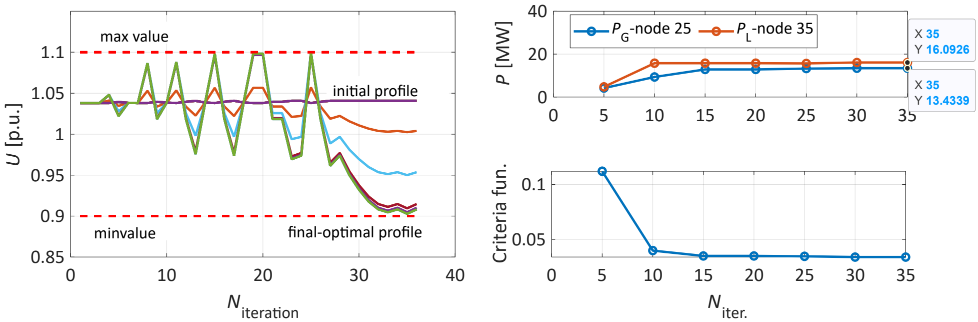

Figure 16: *Voltage profile in all thirty-five nodes while adding a generation unit into node 28 (left) and adding load (right)*

Due to the large number of possible combinations, only one further example is presented, where the two mentioned nodes switched types; so now there is additional load at node 25 and additional production at node 35. The result of the analysis is presented in Figure 16, where the change in the voltage distribution in twenty-five iterations can be seen on the left. This time, some nodes in front of the load node increase in voltage (compared to the results in Figure 14), and similarly, the voltage decreases in the last node where we add production, which is the opposite of the case in Figure 14. In the last iteration, when a satisfactory convergence has already been achieved, we can evaluate both values and conclude that in this case an additional production unit, size $P_{G\text{-}25}$ = 13.43 MW, can be added to node 25, and an additional load to node 35, namely $P_{L\text{-}35}$ = 16.09 MW

4 CONCLUSIONS

An inaccurate and inconsistent assessment regarding the possibility of connecting new elements in the distribution network can have a discriminatory effect on an individual, as their request to connect a new device may be rejected or permitted to a lesser extent than desired. This article presents an integrated approach to network analysis, which is carried out on a real example and verified with real measurements. The treated network already has a few production units as well as larger loads, both of which may increase in the future for objective reasons. The article presents the construction of a model for calculating voltage conditions in the network using standard methods. Verification of the model for any moment in the year is also carried out, so that different scenarios of additional elements in the network can be explored by means of simulation. By random testing and using an unsystematic approach, time-consuming procedures can be replaced by a comprehensive approach, including the use of an optimisation algorithm. The method of differential evolution was used, which finds the maximum value of the search variable for each node at every moment in the year, for either an additional load or an additional unit of production. An upgrade to this is to extend the operation of the network with an OLTC device, which can further improve the voltage profile within the intended limits. Finally, a dual-criteria optimisation is presented, where we simultaneously include both opposing elements in the network, but where, due to nonlinearity and complexity, it is difficult to find the local extrema of the desired function. In the future work, it is possible to upgrade the model to more simultaneous search criteria or to use it as a model example of the entire approach.

References

[1] E. Bompard, E. Carpaneto, G. Chicco, and R. Napoli, *Convergence of the backward/forward sweep method for the load-flow analysis of radial distribution systems*, Electrical Power and Energy Systems 22 (2000) 521–530: Available: https://doi.org/10.1016/S0142-0615(00)00009-0

[2] B. Stott, *Review of Load-Flow Calculation Methods*. Proceedings of the IEEE, 1974. 62(7): pp. 916-929. **Available**: https://ieeexplore.ieee.org/document/1451474

[3] V.V.S.N. Murty, B. Ravi Teja, and A. Kumar, *A Contribution to Load Flow in Radial Distribution System and Comparison of Different Load Flow Methods*. 2014 International Conference on Power Signals Control and Computations (Epscicon), 2014. **Available**: https://ieeexplore.ieee.org/document/6887494

[4] Y. Xiang, J. Liu, F. Li, Y. Liu,, R. Xu, et al. *Optimal active distribution network planning: a review. Electr Power Compo Syst 2016;44:1075–94.* **Available**: https://doi.org/10.1080/15325008.2016.1156194

[5] R.P. Broadwater, A. Chandrasekaran, C.T. Huddleston, A.H. Khan, *Power flow analysis of unbalanced multiphase radial distribution system*, EPSR, 14 (1988), pp. 23-33 **Available**: https://doi.org/10.1016/0378-7796(88)90044-2

[6] R. Hemmati, *Optimal design and operation of energy storage systems and generators in the network installed with wind turbines considering practical characteristics of storage units as design variable, J Clean Prod, 185 (2018), pp. 680-693,* **Available**: https://doi.org/10.1016/j.jclepro.2018.03.062

[7] T. F. Agajie, B. Khan, H. H. Alhelou and O. P. Mahela, *Optimal expansion planning of distribution system using grid-based multi-objective harmony search algorithm*, *Computers Electrical Engineering*, vol. 87 (2020), no. 106823, **Available:** https://doi.org/10.1016/j.compeleceng.2020.106823

[8] Y. Liu, X. Wang, and J. Xiao, *Distribution network reconfiguration based on differential evolution algorithm*, *Proceedings, 3rd Pacific-Asia Conference on Circuits, Communications and System*, art. no. 5990258.(2011), **Available:** https://doi.org/10.1016/j.aasri.2012.11.034

[9] K. Wang, Z. Song, H. Guo, J. Ma, B. Song, Y. Hu, and M. Xu, *Voltage Control Strategy of OLTC-Inverter in Distribution Transformer Area with High-proportion Residential Photovoltaics.* 2022 Power System and Green Energy Conference (PSGEC). 2022 Power System and Green Energy Conference (PSGEC). IEEE. **Available:** https://doi.org/10.1109/PSGEC54663.2022.9881078

Journal of Energy Technology

JET Volume 15 (2022) p.p. 25-36
Issue 3, 2022
Type of article: 1.01
www.fe.um.si/si/jet.html

A COMPANY'S CARBON FOOTPRINT AND SUSTAINABLE DEVELOPMENT

OGLJIČNI ODTIS PODJETJA IN TRAJNOSTNI RAZVOJ

Jure Gramc[1], Rok Stropnik[1], Mitja Mori[1ℜ]

Keywords: Carbon footprint, sustainable development, environmental impacts, GHG Protocol, greenhouse gas emissions, global warming, sensitivity analysis

Abstract

Climate changes are already here. And they will get much worse in time. The main reason for global warming is GHG emissions from anthropological sources. That includes transportation, industry, electricity production, agriculture, and others. The European Union has introduced a new Green Deal as an answer to climate change. The European Green Deal puts more pressure on companies to mitigate their carbon footprint and implement sustainable development. One of the basic steps in the analysis of the environmental profile of a company is the identification of hot spots by using the carbon footprint methodology. The workflow of the carbon footprint calculation follows GHG Protocol standardised methodology. The calculation was made for a medium-sized company in the plastics industry. For all GHG emission sources, hot spots were identified and analysed. Based on the hot spots, sensitivity analysis for different pre-defined scenarios has been made, which are aligned with the company's mid- and long-term sustainability goals. The three main hot spots of the company within scopes 1 and 2 are purchased heat, purchased electricity, and combustion of fuels in company vehicles. GHG emissions of heat and electricity are dependent on their distributor and their electricity and heat sources. The hot spot of scope 3 is purchased goods, especially plastic granulate. In the study, we focus only on scope 1 and scope 2.

ℜ Corresponding author: Dr. Mitja Mori, University of Ljubljana, Faculty of Mechanical Engineering, Aškerčeva cesta 6, Ljubljana, Tel.: +386 41 505 003, E-mail address: mitja.mori@fs.uni-lj.si

[1] University of Ljubljana, Faculty of Mechanical Engineering, Aškerčeva cesta 6, Ljubljana

Povzetek

Podnebne spremembe so že tu in s časom postajajo vse hujše. Glavni razlog za globalno segrevanje so toplogredne emisije iz antropogenih virov. Te vključujejo transport, industrijo, proizvodnjo električne energije, kmetijstvo in ostale. Odgovor Evropske unije na podnebne spremembe je Evropski zeleni dogovor. Ta povečuje pritisk na podjetja za zmanjšanje njihovim toplogrednih emisij in implementacijo trajnostnega razvoja. Eden temeljnih korakov pri analizi okoljskega profila podjetja je identifikacija vročih točk z uporabo metodologije ogljičnega odtisa. Potek izračuna ogljičnega odtisa podaja standardizirana metodologija GHG Protocol. Analiza je narejena za srednje-veliko podjetje iz sektorja plastične industrije. Med vsemi viri toplogrednih emisij so identificirane in analizirane vroče točke podjetja. Glede na identificirane vroče točke je narejena tudi občutljivostna analiza za različne scenarije, ki so v skladu s srednje in dolgoročnimi trajnostnimi cilji podjetja. Vroče točke podjetja znotraj obsega 1 in 2 so toplota, elektrika in uporaba osebnih avtomobilov podjetja. Toplogredne emisije toplote in elektrike so odvisne od distributerja in njegovih virov energije. Najvplivnejša kategorija obsega 3 je kategorija kupljeno blago in storitve, predvsem nakup plastičnega granulata. V študiji se osredotočamo zgolj na obseg 1 in obseg 2.

1 INTRODUCTION

Climate change represents one of the biggest threats to humanity. The Intergovernmental Panel on Climate Change (IPCC) in their last report [1] states that because of the excessive use of fossil fuels, the concentration of greenhouse gases (GHG) in the atmosphere has been increasing since 1750. Today we have the highest level of concentration of GHG emissions of the last 2 billion years. GHG emissions are the main cause of the global warming we are facing today. The last four decades have been the warmest since 1850. Although we are aware of the situation, and according to Kacha et. al. [2] around 94% of Europeans believe that the climate is definitely or probably changing, we do not act. Energy consumption is still rising, according to the International Energy Agency (IEA) [3].

Climate change is not only a threat to our physical environment, but according to Letcher [4], it also causes social injustice and creates climate refugees. Social inequalities continue to increase, and the gap between social classes is widening. More and more people already live in almost uninhabitable areas, from where they migrate to other, more climate-friendly countries. This, unfortunately, causes tensions between people of different cultures, values and races. All this social tension, which is indirectly caused by climate change, further distances us from solving this global crisis.

Global warming is happening due to the change in the equilibrium of energy flows between the Earth and space. With an increased concentration of greenhouse gases in the atmosphere, more energy can be absorbed in the atmosphere, meaning that the greenhouse effect would also increase. Consequently, more energy is held by the atmosphere, and therefore the Earth's climate is warming. The Earth's energy balance is presented in Figure 1.

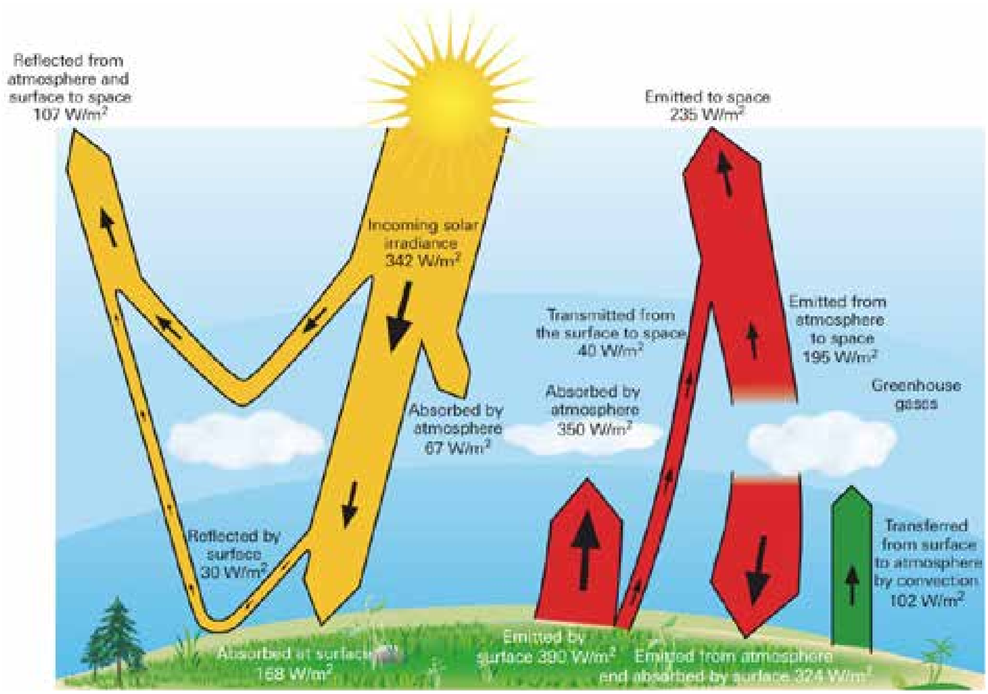

Figure 1: *Earth energy balance, [5]*

One of the biggest reasons why global warming is such a serious problem is the feedback mechanism, fuelling itself when triggered, as is explained by Letcher [4]. And it has already been triggered. The concentration of water vapour, which is an important GHG, is increasing, as ice is melting, making the surface of the Earth less reflective and therefore absorbing more solar radiation, as land and open water takes the place of ice, etc. With the ocean's temperature increasing, less carbon dioxide (CO_2) can be stored within in, which again increases the concentration of CO_2 in the atmosphere. Meaning that even if we stopped emitting GHGs, feedback mechanisms would still continue global warming to some extent. The scientists on the IPCC [1] agree that the point of no return is an increase in global temperature of more than 2°C compared to the pre-industrial average. Scientists believe that if global temperatures increase above 2°C it would cause irreversible changes in the Earth's climate, with it gradually becoming uninhabitable for the human race.

If we want to preserve the human race, countries need to act according to the international climate agreements they signed. The Paris Agreement, and in particular the Glasgow Climate Pact, set up measures for GHG reduction that would slow down and eventually stop global temperature rise. But with the Covid-19 pandemic and the Ukraine-Russia crisis, countries are unlikely to meet these goals and stop this global catastrophe. Nevertheless, the European Union (EU) took a step in the right direction with its new Green Deal, which puts pressure on companies to follow sustainable development guidelines. One of the core sustainable development elements is a company's carbon footprint.

The carbon footprint is a methodology for calculating the GHG emissions made by a company. There are many different definitions of the carbon footprint, as discussed in the study by Wright et. al. [6]. In this paper, the carbon footprint is defined as "A measure of the total amount of GHG emissions determined in the Kyoto Protocol plus NF3 emissions of a defined company, taking into account all relevant sources, sinks, and storage within the spatial and temporal boundary of the company, calculated as CO_2eq using the relevant 100-year global warming potential (GWP100)".

2 GHG PROTOCOL METHODOLOGY

Over time, different methodologies for the calculation of carbon footprint have been defined. Out of the need for a standardised method, so that comparison between different carbon footprints is possible, ISO Standard 14064 [7] was introduced. In this study the GHG Protocol methodology was used, which is defined in the GHG Protocol Corporate Accounting and Reporting Standard [8]. In addition, the Technical Guidance for Calculating Scope 3 Emissions [9] was also used. GHG Protocol methodology is used and recognised worldwide and was used as the basis of ISO Standard 14064.

2.1 Organizational Boundaries

Organizational boundaries are the first step in the GHG Protocol methodology. Organizational structures of companies come in many forms, therefore the definition of organizational boundaries is a necessary and very important step. Two different approaches could be used: the equity share approach and the control approach.

With the equity share approach, the company accounts for GHG emissions from GHG sources based on its share of equity in the operation of the GHG source. The equity share reflects the economic interest of the company.

With the control approach, the company accounts for all GHG emissions from GHG sources over which the company has control. It does not account for GHG emissions from operations in which it owns an interest but has no control. Control can be financial or operational.

2.2 Operational Boundaries

The next step in the GHG Protocol methodology is the definition of operational boundaries. First, all GHG emission sources must be identified, then the GHG sources are categorised as direct or indirect emissions and put into a suitable scope. Direct GHG emissions are emissions from sources that are owned or controlled by the company. Indirect GHG emissions are emissions that are a consequence of the company's activities but occur at sources owned or controlled by another company.

As is shown in Figure 2, in GHG Protocol three scopes are defined: scope 1, scope 2, and scope 3. Scope 1 includes direct emissions. The most common GHG sources within scope 1 are generation of electricity, heat or steam; physical or chemical processing; transportation of materials, products, waste and employees; and fugitive emissions.

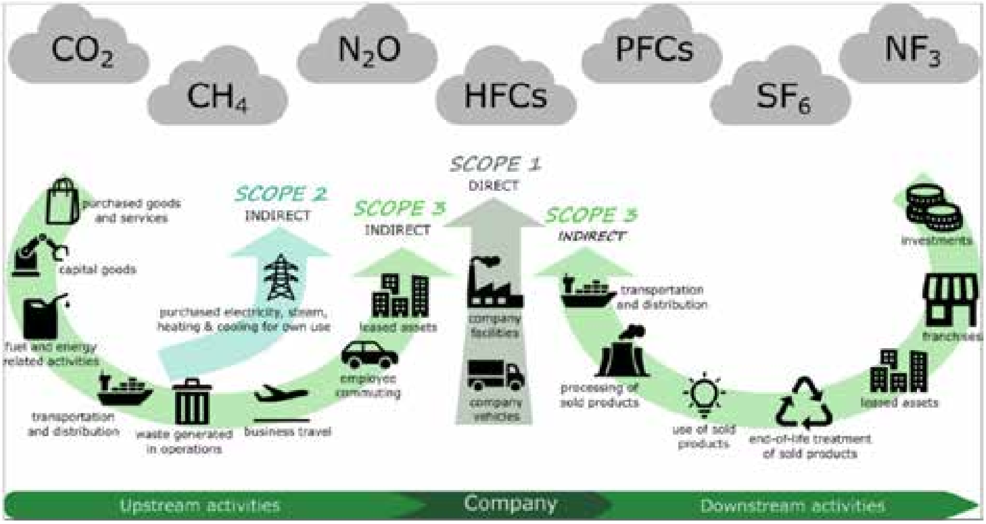

Figure 2: *Scopes of Carbon Footprint,* [9]

Scope 2 includes indirect GHG emission sources from purchased electricity, heat or steam. Electricity, heat or steam are consumed by the company, but the generation of electricity, heat or steam, and therefore its GHG emissions, do not occur within the company, but somewhere else.

Scope 3 includes all other indirect emission sources. They are divided into 15 categories, as presented in Figure 2. Scope 3 GHG emission sources are a consequence of the company's activities, but they are not owned or controlled by the company.

Indirect GHG emissions are divided into two scopes (scope 2 and scope 3), of which only scope 2 is mandatory to report (along with the direct GHG emissions of scope 1, of course). Scope 3 is optional, as the company does not have full control over these GHG sources. Therefore, the company has limited data that is needed for carbon footprint calculation. Also, the intensity of GHG emissions for each category varies from company to company. In contrast, GHG emission sources in scope 2 are very common, and almost every company purchases electricity or heat. Data for calculation of scope 2 GHG emissions is also easy to acquire because the distributor must state the energy sources of the electricity or heat provided.

2.3 Base Year

The company may need to track GHG emissions over time to compare carbon footprint over time, establish GHG targets, or for other reasons. To be able to make a meaningful and consistent comparison of GHG emissions over time the base year GHG emissions must be set. The company should choose the earliest relevant point in time for which they have reliable data as the base year. For consistent tracking of GHG emissions over time, the base year GHG emissions may need to be recalculated, as companies undergo significant structural changes, such as acquisitions, divestments and mergers.

3 ASSESSMENT OF CARBON FOOTPRINT IN A COMPANY

The workflow of the carbon footprint methodology is presented in Figure 3. The most time-consuming step is collecting data and choosing suitable emissions factors. Red arrows represent feedback loops that occur if there is no data or the quality of the data is not sufficient. With feedback loops, we ensure relevance, completeness and transparency.

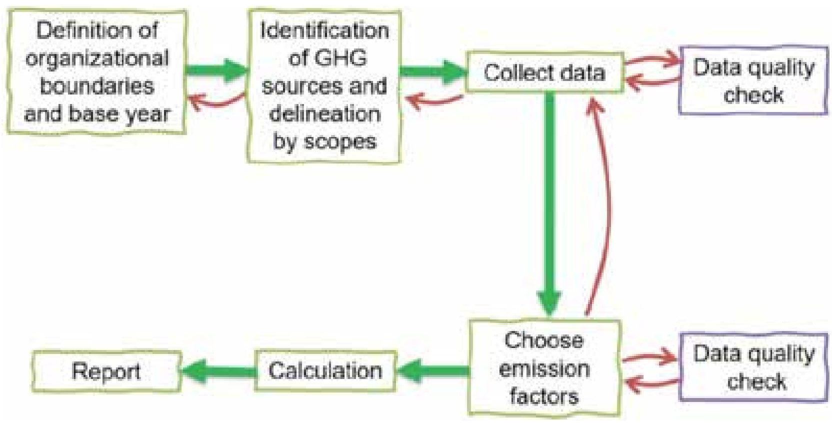

Figure 3: *Workflow of the carbon footprint methodology*

3.1 Boundary Conditions

A carbon footprint was made for a medium-sized company in the plastics industry. The year 2019 was chosen as the base year. We calculated only the base year's carbon footprint. Setting the organizational boundaries was very straightforward, as the company is located in only one place, where it has offices and production halls, and they do not have any joint operations. To define the organizational boundaries, we used the control approach.

3.2 Identification of GHG Sources

GHG emission sources for scopes 1 and 2 are presented in Table 1. GHG emission sources within scope 1 include vehicles and fugitive emissions. The company has passenger cars, delivery vehicles and forklifts. All of the passenger cars and delivery vehicles run on diesel, while one forklift is diesel, two run on liquefied petroleum gas (LPG), and the rest are electric. The company's fugitive emissions consist of refrigerants from cooling and air conditioning systems. All of them undergo annual checks. In the base year, leaking of only one refrigerant was detected. From one of the cooling systems, 8 kg of refrigerant R410A was emitted into the environment.

GHG sources within scope 2 are electricity consumption and district heating consumption. The company purchased electricity from a hydro energy source, while the energy source of district heating is lignite. Heat is provided from a cogeneration heat and power (CHP) plant.

Table 1: *GHG emission sources for scope 1 and scope 2*

GHG Sources	**Base year (2019)**
SCOPE 1	
Vehicles consumption	
Diesel [L]	22200
Passenger cars [L]	15200
Delivery vehicles [L]	4400
Forklifts [L]	2600
LPG – forklifts [kg]	2000
Fugitive emissions	
Refrigerant – R410A [kg]	8
SCOPE 2	
Electricity consumption [kWh]	7025
District heating consumption [MWh]	380

GHG emissions of scope 3 are not discussed in this study, although a calculation of scope 3 emissions has been made. The calculation includes the following scope 3 categories: purchased goods and services, upstream and downstream transportation and distribution, waste generated in operations, business travel, and employee commuting.

3.3 Uncertainty

The uncertainty of the carbon footprint calculation depends on the uncertainty of emissions factors and the uncertainty of activity data. Emissions factors are used from official databases, and therefore uncertainty is relatively small. Emissions factors from databases represent average processes for a specific nation or region. The use of averaged data and not specific data for processes is the biggest source of uncertainty of emissions factors. With additional checks of emissions factors, we make sure that the most appropriate emissions factor is selected, which means that the uncertainty is as low as possible.

The second uncertainty is the uncertainty of activity data. While the company owns all the processes, activity data has negligible uncertainty. Uncertainty of activity data is mostly due to uncertainty of measuring equipment and data processing within the company.

Overall, uncertainty for scopes 1 and 2 is small. The company has first-hand activity data, which has negligible uncertainty, and second-hand emissions factors, which are taken from official databases. Uncertainty of emissions factors could be lower if specific processes would be included in the databases.

Uncertainty of scope 3 is much bigger than the uncertainty of scopes 1 and 2, as the activity data is second-hand and often averaged, estimated, and generalised. Therefore, activity data is the main source of uncertainty for scope 3, as the databases from which emission factors are used remain the same. The high uncertainty in scope 3 is one of the reasons why scope 3 is optional and is not included in this study.

4 RESULTS

In this section, carbon footprint results for scope 1 and scope 2 are presented for a medium-sized company in the plastics industry. Along with the results of the carbon footprint, which are presented in Table 2, we analyse and identify hot spots in scopes 1 and 2. Additionally, sensitivity analysis is also presented for various scenarios that could be implemented in the company and have the potential to reduce the carbon footprint.

Table 2: *The carbon footprint of scope 1 and scope 2*

GHG Sources	**Carbon footprint [t CO_2 eq.]**
SCOPE 1	**76.5**
Vehicles	61.1
Passenger cars	40.7
Delivery vehicles	11.8
Forklifts	8.6
Fugitive emissions – R410A	15.4
SCOPE 2	**159.8**
Electricity consumption	38.2
District heating consumption	121.6
TOTAL SCOPE 1 AND SCOPE 2	**236.3**

As presented in Table 2, scope 2 has a much bigger carbon footprint than scope 1. The carbon footprint of scope 1 is 76.5 t CO_2 eq., while the carbon footprint of scope 2 is 159.8 t CO_2 eq., which represents a 108% increase in carbon footprint. The total carbon footprint of scopes 1 and 2 is 236.3 t CO_2 eq., which is negligible compared to the scope 3 carbon footprint, which is 17915.5 t CO_2 eq. The carbon footprint of scopes 1 and 2 represent only 1.3% of the carbon footprint of scope 3.

4.1 Hot spots

Proportions of GHG emission sources are presented in Figure 4. By far the biggest source of GHG emissions is district heating consumption, which is responsible for 51% of the scope 1 and 2 carbon footprint. The reason for such high GHG emissions is the energy source of the district heat, which is lignite.

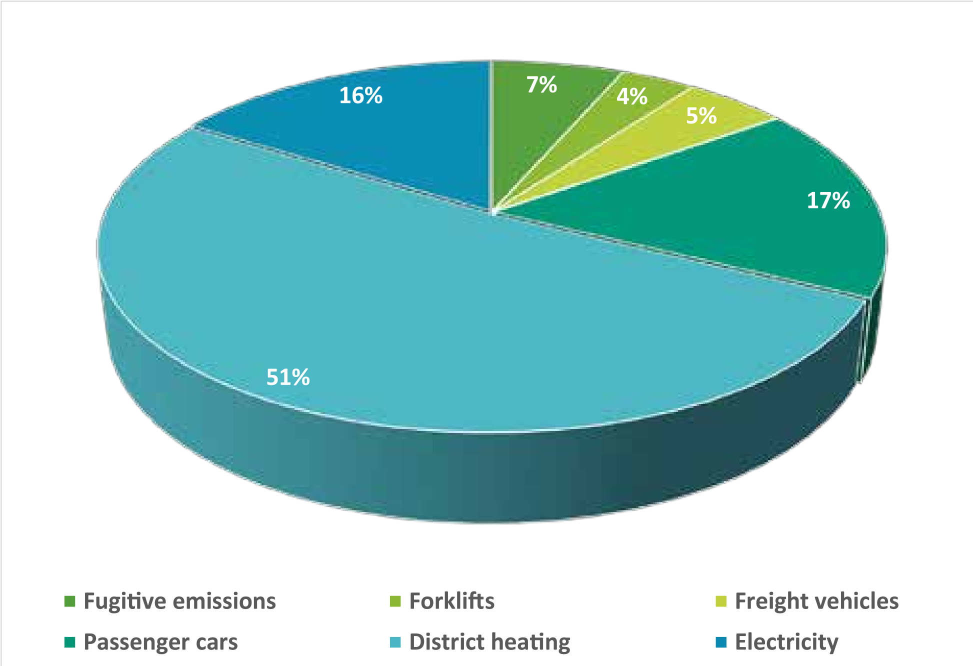

Figure 4: *GHG emission sources of scope 1 and scope 2*

If district heating is the hot spot of scope 2, the hot spot of scope 1 is passenger cars. Passenger cars are responsible for 53% of the carbon footprint of scope 1 and 17% of scopes 1 and 2. All the passenger cars are diesel. Other activities in scope 1 represent only small proportions of the carbon footprint.

Among noticeable activity is also electricity. It is responsible for 16% of the carbon footprint of scopes 1 and 2, which is almost the same as for passenger cars. Considering the amount of purchased electricity, its carbon footprint is really small. The reason for this is the source of electricity, which is hydro energy, one of the most carbon-neutral energy sources.

The hot spot of scope 3 is purchased goods and services, more precisely, purchases of plastic granulate. Plastic granulate is responsible for 86% of the carbon footprint of scope 3 and is the main reason why scope 3 GHG emissions are so high.

4.2 Sensitivity analysis

Different mitigation strategies that could be implemented by the company to reduce its carbon footprint of scopes 1 and 2 were analysed. Mitigation strategies are presented in the paper as activities A, B, C, D and E. After recalculation of the carbon footprint for each activity, a sensitivity analysis was conducted, analysing which activities contribute the most to GHG emission reduction. Results of the sensitivity analysis are presented in Figure 5.

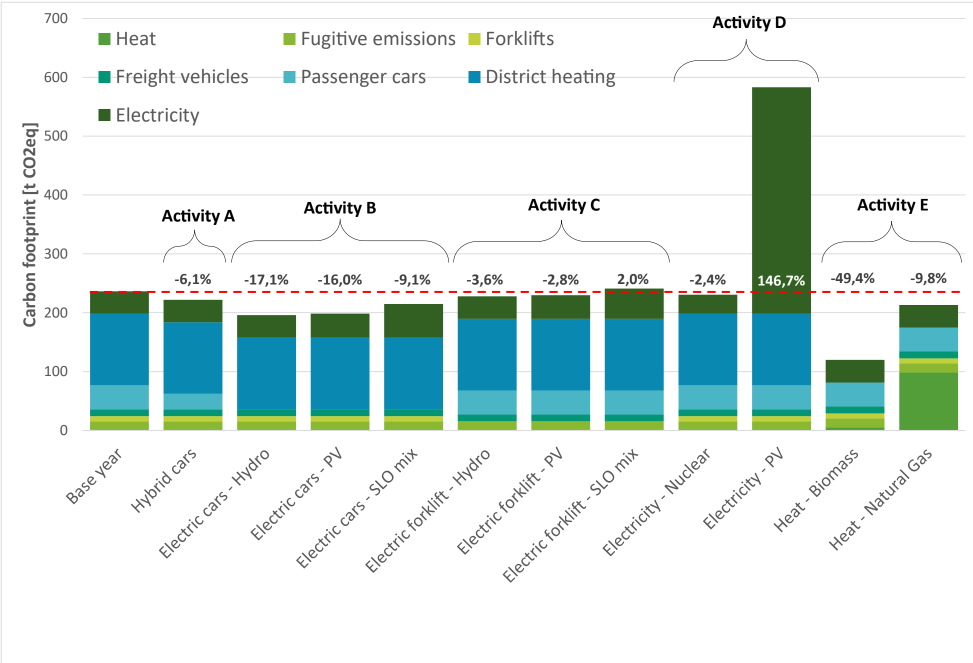

Figure 5: *Mitigation activities of carbon footprint for scopes 1 and 2*

The base scenario is the scenario for which we calculated the carbon footprint. Activity A substitutes diesel passenger cars with hybrid passenger cars. The emissions factor for the average hybrid car is taken from the DEFRA database [10]. Activity A contributes to a carbon footprint reduction of 14.4 t CO_2 eq., which means that the carbon footprint of scopes 1 and 2 would decrease by 6.1%.

Activity B is the electrification of diesel passenger cars. We compare the carbon footprint of electric cars for different electricity sources: hydro energy, PV energy, and the Slovenian electricity grid mix. We assume the power consumption of electric cars to be 22.5 kWh/100 km. With the use of hydroelectricity, the reduction in carbon footprint is 40.4 t CO_2 eq., which equals 17% of the carbon footprint of scopes 1 and 2. Similar reductions can be seen in the case of PV electricity. In this case, it is reduced by 37.9 t CO_2 eq., which is equivalent to 16% of the carbon footprint of scopes 1 and 2. For the Slovenian electricity grid mix, reductions are smaller, and only 21.5 t CO_2 eq. is mitigated, which equals 9% of the carbon footprint of scopes 1 and 2. If activity B was implemented, GHG emissions of scope 1 would drastically decrease, while scope 2 emissions would increase, because of the increase in electricity consumption.

Activity C is the electrification of diesel and LPG forklifts. We used the same electricity sources as in activity B. We assume that three electric forklifts would be needed, which are charged once a day and use 30 kWh of energy per charging. With hydroelectricity, GHG emission reduction is 8.4 t CO_2 eq. which equals 4% of the carbon footprint of scopes 1 and 2. Even smaller reductions are seen in the case of PV electricity, where only 6.7 t CO_2 eq. is reduced, which equals 3% of the carbon footprint of scopes 1 and 2. If the company electrified forklifts and used the Slovenian electricity grid mix then the carbon footprint of the company would increase by 4.6 t CO_2 eq. As in activity B, if activity C is implemented GHG emissions fall within scope 2.

Activity D is a comparison of different electricity sources. We compare hydro energy (base scenario), nuclear energy and PV energy. The nuclear energy source has slightly lower GHG emissions than hydro energy, meaning that the company could have a minimal reduction in carbon footprint if they used nuclear power electricity. The reduction would be 5.7 t CO_2 eq., which is equivalent to 2% of the carbon footprint of scopes 1 and 2. If the company uses electricity from PV energy then the carbon footprint would increase by 346.8 t CO_2 eq., equivalent to a 147% increase in the carbon footprint of scopes 1 and 2. Although this seems like a big increase, and it is, it would be even worse if the company used a Slovenian grid mix. In that case, the increase of carbon footprint would be 2596.2 t CO_2 eq., which is a 1099% increase in the carbon footprint of scopes 1 and 2. Even more worrying is the fact that the Slovenian grid mix is below the European average [11].

Activity E is a comparison of different heat sources. We compare district heating on lignite from the CHP power plant (base scenario), local furnace on biomass, and local furnace on natural gas. Local furnace on biomass would reduce GHG emissions by 116.7 t CO_2 eq., which equals a 49% decrease in the carbon footprint of scopes 1 and 2. Reduction in the case of a local furnace on natural gas is a bit lower, 23.2 t CO_2 eq., which is a 10% decrease of the carbon footprint of scopes 1 and 2. If the company implemented activity with a local furnace, GHG emissions would fall within scope 1.

As is presented in Figure 5, by far the biggest reduction is achieved by activity E. Local furnace on biomass could reduce GHG emissions by almost 50%. The second biggest reduction is the electrification of passenger cars. Reductions are dependent on the type of electricity; the biggest reduction occurs with hydro energy sources and PV energy sources. The Slovenian electricity grid mix achieves some reductions, but they are still high compared to other activities. Activities A, C and D have relatively small impacts (below 7%), therefore the implementation of these activities does not have a big impact on the mitigation of carbon footprint. If we implemented all the most optimistic versions of the activities, the company could reduce its carbon footprint by 55%.

Scenario analysis considers purely theoretical implementations of activities. Technical and economic aspects of the implementation of activities are not considered in this study.

5 CONCLUSIONS

In the paper, the GHG Protocol methodology and calculation of carbon footprint for a middle-sized company in the plastics industry is assessed. The calculation is made for all three scopes with additional scenario analysis for five mitigation activities. Although scope 3 represents the vast majority of GHG emissions, the emphasis is on mitigation of scope 1 and scope 2 activities, because the company has more control over these activities.

Activity data needed for calculation for scopes 1 and 2 is provided by the company, therefore the uncertainty of the data is small. Emissions factors from official databases were used, which have relatively small uncertainty. Therefore, the uncertainty of the scope 1 and scope 2 calculation of carbon footprint is fairly small. On the other hand, the uncertainty of scope 3 is high, as the activity data is not gathered within the company but from partners of the company. Data is often averaged, estimated, and generalised, which is one of the reasons for high uncertainty.

The greatest GHG emission reductions are achieved with activity E – local furnace on biomass. Some reductions are also achieved with activity B – electrification of passenger cars with a hydro energy source. Other activities have much smaller impacts on the mitigation of carbon footprint. If we implemented all the most optimistic versions of the activities, the company could reduce its carbon footprint by 55%.

The carbon footprint is one of the most important tools for fighting global warming. If we want to mitigate the effects of climate change, a carbon footprint policy should be mandatory for all companies. It is expected that it will be implemented into European Union legislation in the future. Until then, carbon footprint is only on the agenda of sustainability-oriented companies, companies that are motivated by their distributors, or companies that are already oriented towards the future.

References

[1] **Intergovernmental Panel on Climate Change**, *Climate Change 2021: The Physical Science Basis*, 2021

[2] **O. Kácha, J. Vintr, C. Brick**: *Four Europes: Climate change beliefs and attitudes predict behavior and policy preferences using a latent class analysis on 23 countries*, Journal of Environmental Psychology, Vol. 81, 2022

[3] "International Energy Agency–Data and statistics." https://www.iea.org/data-and-statistics/data-browser/?country=WORLD&fuel=CO_2 emissions&indicator=TotCO_2 (04. 09. 2021)

[4] **T. M. Letcher**: *Climate Change*, Elsevier, 2021

[5] **I. S. F. Jones**, *Geoengineering the climate: science, governance and uncertainty*. London: Royal Society, 2009

[6] **L. A. Wright, S. Kemp, I. Williams:** *'Carbon footprinting': Towards a universally accepted definition*, Carbon Management, Vol. 2, p.p. 61–72, 2011

[7] *Toplogredni plini–1.del: Specifikacija z navodilom za količinsko določanje in poročanje o emisijah in odstranjevanju toplogrednih plinov na ravni organizacije (ISO 14064-1:2018)*.

[8] **World Business Council for Sustainable Development and World Resources Institute:** *The Greenhouse Gas Protocol: A Corporate Accounting and Reporting Standard,* 2012

[9] **World Business Council for Sustainable Development and World Resources Institute:** *The Greenhouse Gas Protocol: Technical Guidance for Calculating Scope 3 Emissions*, 2013

[10] "Greenhouse gas reporting: conversion factors 2021–GOV.UK." https://www.gov.uk/government/publications/greenhouse-gas-reporting-conversion-factors-2021 (29. 07. 2022)

[11] "Electricity Mix–Our World in Data." https://ourworldindata.org/electricity-mix (10. 08. 2022)

Journal of Energy Technology

JET Volume 15 (2022) p.p. 37-52
Issue 3, 2022
Type of article: 1.01
www.fe.um.si/si/jet.html

USE OF ACTIVE ELEMENTS FOR PROVIDING SUITABLE VOLTAGE PROFILES AND PREVENT OVERLOADS IN RADIAL DISTRIBUTION NETWORKS

UPORABA AKTIVNIH ELEMENTOV ZA ZAGOTAVLJANJE USTREZNIH NAPETOSTNIH PROFILOV IN PREPREČEVANJE PREOBREMENITEV V RADIALNIH DISTRIBUCIJSKIH OMREŽJIH

Marko Vodenik[1ℜ], Matej Pintarič[1], Gorazd Štumberger[1]

Keywords: voltage profile, radial distribution network, load flow calculations, active network elements, energy flexibility

Abstract

The article deals with the issue of providing suitable voltage profiles and preventing congestion of network elements in distribution networks. Active network elements and network users' energy flexibility services are used to provide a suitable voltage profile and prevent congestion in distribution networks. The discussed active network elements include a transformer with on-load tap changer, reactive power compensation devices, energy storage systems, distributed energy

ℜ Corresponding author: M.Eng., Marko Vodenik, University of Maribor, Faculty of Electrical Engineering and Computer Science, Koroška cesta 46, 2000 Maribor, Tel.: +386 2 22 07 180, E-mail address: marko.vodenik1@um.si

[1] University of Maribor, Faculty of Electrical Engineering and Computer Science, Koroška cesta 46, 2000 Maribor

resources, and network users' energy flexibility services, where the active consumers adjust their consumption, production and storage of energy. Based on the Backward Forward Sweep load flow computation method, the case studies are performed for the discussed low voltage distribution network, where the measurement results were available. The case studies for preventing overload of the distribution transformer are performed using a battery energy storage system and network users' energy flexibility services. The case studies for providing suitable voltage profiles are performed using all listed active elements and a combination of different active elements. In addition, to provide suitable voltage profiles, the existing conductors are replaced with conductors of a larger cross-section. Technically acceptable solutions that can provide a suitable voltage profile and prevent the overloading of network elements in the most demanding operating conditions are presented in this article.

Povzetek

V članku je obravnavana problematika zagotavljanja ustreznih napetostnih profilov in preprečevanje preobremenitev elementov omrežja v distribucijskih omrežjih. Za zagotavljanje ustreznega napetostnega profila in preprečevanje preobremenitev v distribucijskih omrežjih so uporabljeni aktivni elementi omrežja in storitev prožnosti energije uporabnikov omrežja. Analize so izvedene z izračunom pretokov energije z uporabo metode *Backward Forward Sweep* za obravnavano nizkonapetostno distribucijsko omrežje, za katero so bili podani rezultati meritev. Izvedeni so bili izračuni preprečevanja preobremenitve transformatorja z baterijskim hranilnikom energije in storitvijo prožnosti uporabnikov omrežja. Izračuni zagotavljanja ustreznega napetostnega profila so bili izvedeni z vsemi naštetimi aktivnimi elementi omrežja in s kombinacijo različnih aktivnih elementov. Zagotavljanje ustreznega napetostnega profila je bilo dodatno izvedeno z zamenjavo obstoječih vodnikov z vodniki večjega preseka. V članku so podane tehnično sprejemljive rešitve z aktivnimi elementi omrežja in s storitvijo prožnosti energije, ki preprečijo preobremenitev elementov omrežja in zagotovijo ustrezen napetostni profil.

1 INTRODUCTION

The increased growth of electricity consumption, especially peak loads, and the integration of DER (distributed energy resources) into the network, can occasionally lead to overloading of individual network elements, such as lines and transformers, and problems in providing suitable voltage profiles. These problems occur mainly in radial distribution networks, due to the network structure and load profile. The properties of radial structured distribution networks are presented in [2].

With active network elements and energy flexibility services, the problems of violation of prescribed voltage profile values and overloading of network elements can be eliminated within certain limitations. In other cases, upgrading and expansion of the network is used, which means the installation of conductors with a larger cross-section and transformers with a higher rated power. The BFS (Backward Forward Sweep) method is used for load flow calculations, which is suitable for radial network calculations. The principle of the BFS method is described in [1].

2 ACTIVE NETWORK ELEMENTS

Active network elements are elements that can be used to change certain parameters in the network, with the aim of providing appropriate and stable operation of the power network. Operational distribution network parameters, such as voltages and energy flows, can be affected with active network elements. Some of the active network elements are: a transformer with OLTC (On-load tap-changer), reactive power compensation devices, ESS (energy storage systems), DER and the network users' energy flexibility services, where the active consumer adjusts the consumption, production and storage of energy.

A transformer with an OLTC can adjust the transformer's ratio, and thus the voltage, whenever the voltage controller detects a secondary voltage that deviates from a predetermined value. Normally there is a voltage control within ±10% of the nominal voltage. This range is divided into nine fixed steps which enable changes of voltage by 2.5% with each step. The operating principle of the transformer with OLTC is described in [3].

Due to a large number of inductive consumers (electric motors, transformers) in the power network, reactive components of the current additionally load the network elements. This phenomenon can lead to undervoltage or overvoltage in distribution networks. The reactive power compensation devices, such as shunt and series compensators, can locally and effectively cover reciprocal energy exchange demand on the consumer side. The principle of reactive power compensation and reactive power compensation devices are described in [4] and [5].

In distribution networks, the use of ESS can improve the stability and reliability of the network. Electrical energy from the network or a DER is converted and stored in an ESS and used later when needed. During times of higher production and lower consumption, excess electrical energy can be stored for a certain period and used when there is lower production and higher consumption in the network. Different methods of energy storage are described in [6]. For use in distribution networks, a BESS (battery energy storage system) is currently the most suitable. Important parameters for choosing a BESS are nominal capacity, power, the battery management system and the type of batteries used to store energy. Different types of BESS are described in [7].

DER is nowadays integrated in almost all distribution networks. Most of them are in the form of renewable energy sources, such as PV (photovoltaic) power plants, wind power plants, biomass energy, geothermal energy, etc. With DER, energy flow in network can be impacted by adjusting the production of active and reactive power. Some of the DER and their impact in distribution networks are described in [8], [9] and [10].

The network users' energy flexibility service represents a new concept where passive consumers of electricity become active consumers – prosumers who can adjust the consumption, production and storage of electricity. With flexibility, it is possible to solve problems of balance of production and consumption of electricity and thus prevent network overloads or provide a suitable voltage profile. The prosumer would, on demand, adjust their consumption, production and storage of electricity to ensure the stable operation of the network. The concept of flexibility and the inclusion of a prosumer in the electricity market is described in [11].

3 DISCUSSED DISTRIBUTION NETWORK

The LV (low voltage) distribution network, for which the measurement results were given, is discussed. A transformer substation (TS) feeds the discussed radial network. It contains three feeders with nineteen connected consumers. Figure 1 shows the diagram of the discussed network. In Figure 1 it can be seen that this network has thirty-nine nodes and thirty-eight branches. Nodes with a consumer are in blue, sections of conductors which are intended to be replaced are in green.

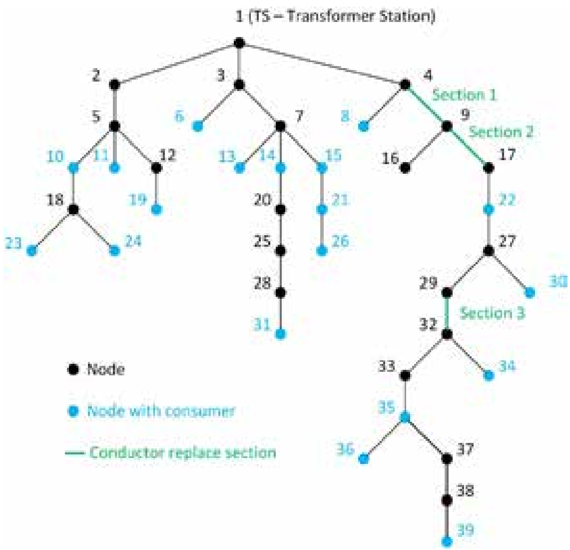

Figure 1: *Diagram of discussed network*

The corresponding installed power of the consumers and the rated power of the transformer in the TS are stated in Table 1.

Table 1: *Installed power of consumers and associated nodes.*

Node	1 (TS)	6	8	10	11	13	14	15	19	21
Installed power [kW]	100 kVA	43	14	14	17	6	17	17	17	17
Node	22	23	24	26	30	31	34	35	36	39
Installed power [kW]	17	17	6	14	17	17	17	17	17	5

4 ANALYSIS

The article deals with two problems, namely transformer overload and violation of the prescribed voltage profile values in the discussed radial distribution network. For each problem a different solution method was used. All calculations were performed in MATLAB.

To prevent transformer overload, the rated data of the transformer was checked. Rated power of the discussed transformer is 100 kVA, as shown in Table 1. Based on the measurement results, it was determined as to whether the transformer was overloaded in any of the observed 15-minute time intervals. For the day with the highest consumption, transformer overload is prevented by employment of active elements and energy flexibility services. In the 15-minute time interval, when the transformer would be overloaded, the necessary active power was generated by the BESS in order to prevent overloads. Another way to prevent overloads in the transformer was the utilisation of network users' energy flexibility services in the form of peak shaving.

To provide a violation of the prescribed voltage profile limits, a network model suitable for load flow calculations was prepared. The model input data were the results of measurements on the transformer, the data of the customers' installed power and load profiles, as well as the parameters of all lines in the discussed network. The topology of the discussed network used in the BFS based load flow calculations is shown in Figure 1. The BFS load flow method [1] is used to determine the voltages in all nodes of the discussed network. Based on the results of load flow calculations, the nodes, in which the voltage profile limits are violated, were identified. In the identified nodes, active network elements, energy flexibility services provided by the network users, and the replacement of unsuitable network elements were all used to prevent violation of the voltage profile.

5 RESULTS

Based on the measurement results, which were available for the transformer in the TS, load flow calculations were performed to solve the problem of overloading and provide a suitable voltage profile with active elements. Measurement results data on the transformer were for the voltage of all three phases, active and reactive power, and were given as 15-minute readings.

5.1 Transformer overload

When reviewing the measurement results for years 2018 and 2019, the transformer in the TS was not overloaded at any time. Therefore, for the purposes of the analysis, a linear 2% annual growth in consumption based on the measurement results was assumed. A calculation was made about what the consumption would be after 30 years, that is, in 2049. The consumption increased by 81.14% compared to the baseline data. With these calculated data, an attempt was made to prevent transformer overload with the BESS and network users' energy flexibility service for the day with highest consumption, which was 22.4.2019. Figure 2 shows the apparent power of the measurement results for the day with the highest consumption (year 2019) and calculated data after linear 2% annual growth in consumption for 2049.

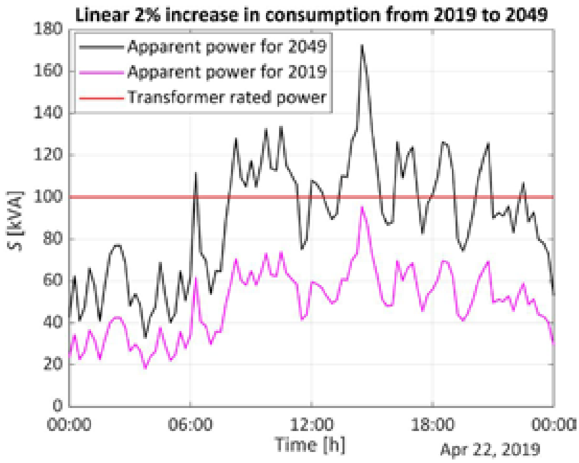

Figure 2: *Apparent power over time for 2019 (pink curve) and for 2049 (black curve)*

5.1.1 Usage of BESS

Under assumptions that the BESS operates between 20% and 80% of nominal capacity, and it was discharged the previous day, it was calculated that a BESS with a minimum nominal capacity of 248 kWh at nominal power of 72.61 kW is needed to prevent overload of the transformer. Figure 3 shows the SOC (state of charge), charging and discharging power of the BESS. It was considered that the BESS is a consumer of electricity while it is being charged and that it generates active power while it is being discharged. In Figure 3b, the blue curve shows charging when the BESS receives active power from the network, and the red curve shows discharging when the BESS outputs active power to the network.

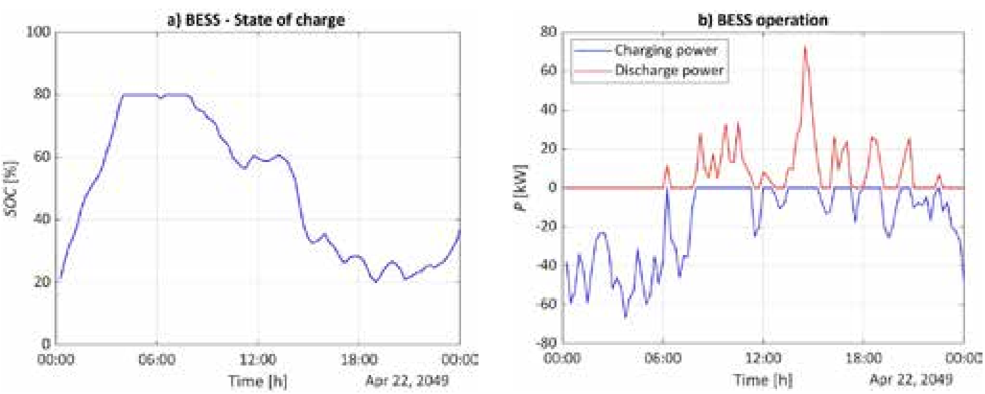

Figure 3: *SOC (a) and operation of BESS (b) over time*

5.1.2 Usage of network users' energy flexibility service

To be able to use the network users' energy flexibility service, the amount of energy that flows through the transformer in an overloaded state and how much energy and power is available to perform flexibility services was calculated. The energy of the overloaded state, in the form of active power with the corresponding share of reactive power was moved to moments when the transformer was not overloaded. The participation of all consumers in the considered network was taken into account. The selected time interval for the flexibility service lasted from 07:00 to 22:00, so that consumption was not shifted to the early morning or night hours. Figure 4 shows the apparent power of the transformer over time and the use of the flexibility service over a 15-hour interval. Transformer overload was not prevented, because after using the flexibility service, the transformer was still overloaded at certain times, as shown by the blue curve in Figure 4.

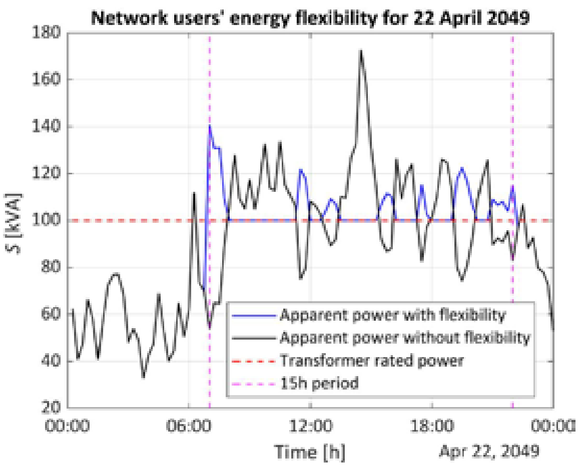

Figure 4: Apparent power over time and use of flexibility service

5.2 Providing a suitable voltage profile

When reviewing the measurement results, the voltages of all three phases at the transformer terminals were within the permissible limits. Based on the network data, a network model was prepared, and load flow was calculated using the BFS method [1]. Voltage profiles for all nodes for the day and the moment of highest consumption were calculated. Figure 5 shows the voltage profile over time and nodes for the day with the highest consumption. The point of highest consumption is at 14:30 on 22.4.2019. Figure 6 shows the voltage profile over nodes for the moment of highest consumption. It was discovered that undervoltage occurs at the end of the third feeder. With this data, an attempt was made to provide a suitable voltage profile with all listed active elements of the network.

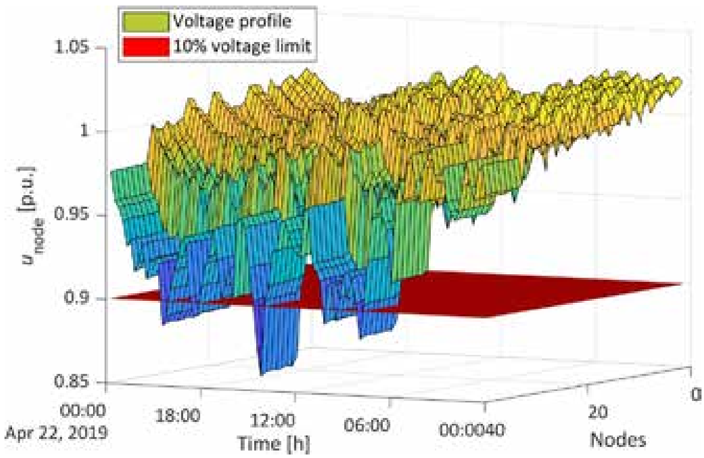

Figure 5: *Voltage profile over time and nodes for the day with highest consumption*

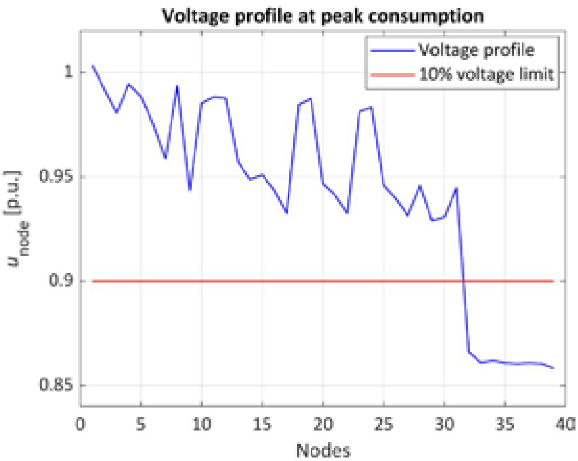

Figure 6: *Voltage profile over nodes for the moment of highest consumption*

5.2.1 Usage of transformer with OLTC

Using a transformer with OLTC, voltage on the secondary side of the transformer was raised by 2.5% and 5%. Standard distribution transformers have five steps, which enable voltage adjustment in the range of ±2 × 2.5% U_n. It was assumed that the transformer is currently set on the mid tap. Figure 7 shows the node-wise voltage profile using a transformer with OLTC with balance node voltage increased. When raising the voltage of the balance node (node 1) by 5%, a suitable voltage profile is provided, which is shown by the pink curve in Figure 7.

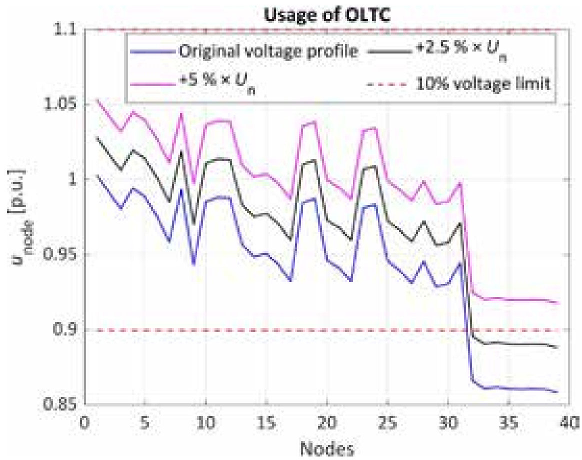

Figure 7: *Voltage profile when the voltage of the balance node is increased*

5.2.2 Use of a reactive power compensation device

Reactive power of a capacitive character was generated with a reactive power compensation device. The location of the compensation device was determined in the third feeder from the TS in which the undervoltage occurred. A undervoltage location at node 27 was determined. The calculations were performed for different power levels of the compensation device. Figure 8 shows the node-wise voltage profile with reactive power compensation at node 27. A suitable voltage profile was not provided.

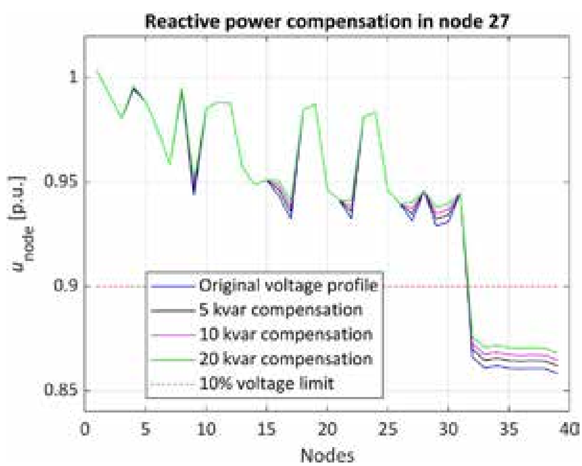

Figure 8: *Voltage profile with reactive power compensation device*

5.2.3 Usage of BESS

With the BESS, active power was generated while the BESS was discharging. While charging, the BESS responded as a consumer of electricity. BESS charging was implemented from 00:00 to 06:00. Discharge of the BESS was done as necessary to provide a suitable voltage profile. The BESS location was chosen in the same node as for the reactive power compensation device. It was calculated that a BESS with a minimum nominal capacity of 29 kWh at a nominal power of 8 kW is needed to provide a suitable voltage profile. To charge the BESS, a charging power of 3.5 kW is required. Figure 9 shows the SOC, charging and discharging power of the BESS at node 27. Figure 10 shows the voltage profile over time and nodes with a BESS installed at node 27. The results clearly show that a suitable voltage profile is provided.

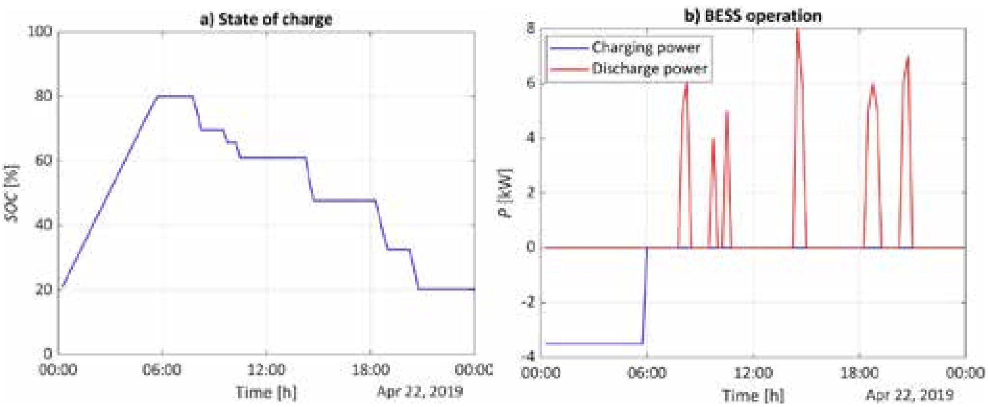

Figure 9: *SOC (a) and operation of BESS (b) at node 27 over time*

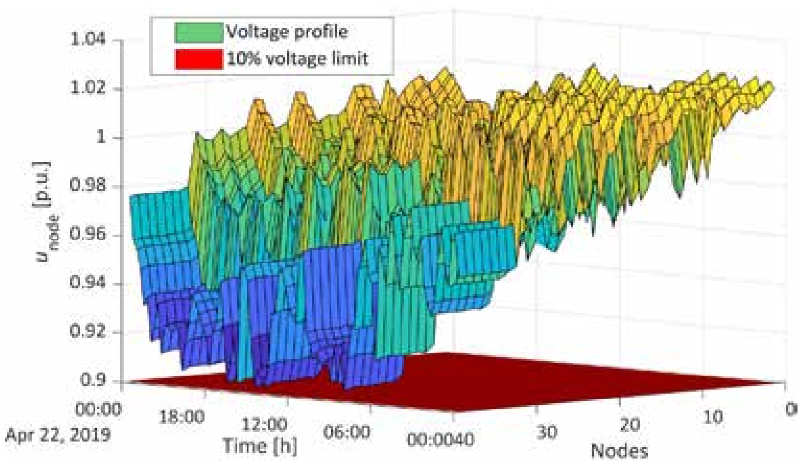

Figure 10: *Voltage profile over time and nodes with BESS at node 27*

5.2.4 Usage of PV power plant

A PV power plant enables the production of active or reactive power. Since it was found in subsection 5.2.2 that it is not possible to provide a suitable voltage profile with reactive power compensation, the PV power plant will generate only active power. It was considered that the power plant is installed at node 35. Based on [12], the maximum power of a PV power plant in the Slovenian distribution network can be up to 80% of the customer's installed power. The installed power of the customer at node 35 is 17 kW, which means that the maximum power of the PV power plant can be up to 13.6 kW. Based on solar irradiation data for 22.4.2019, the output power of the PV power plant was calculated. All the output power was fed into the network to provide a suitable voltage profile. Figure 11 shows the power output profile of the PV plant for the whole day. Figure 12 shows the voltage profile over time and nodes, using the PV power plant installed at node 35. The results show that a suitable voltage profile cannot be provided.

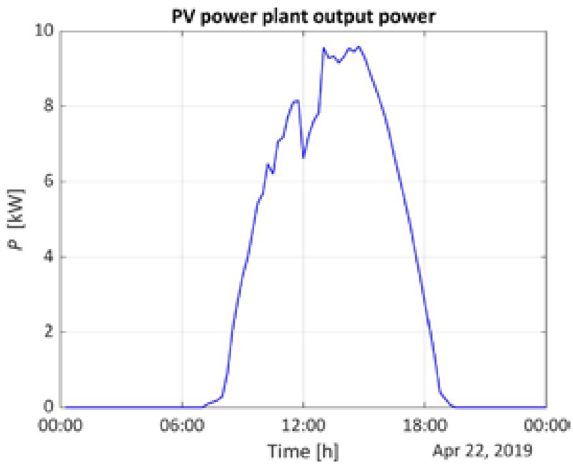

Figure 11: *Output power profile of PV power plant over time*

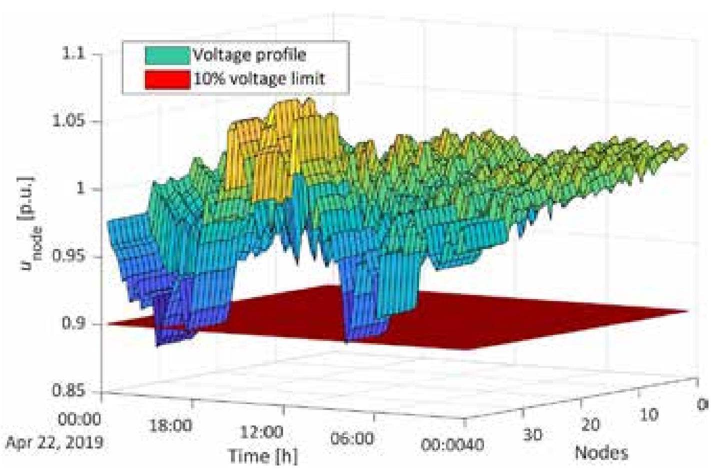

Figure 12: *Voltage profile over time and nodes with PV power plant installed at node 35*

5.2.5 Use of a combination of BESS and PV power plant

In section 5.2.4, it was found that a suitable voltage profile is not provided by using a PV power plant only. Therefore, a combination of the BESS and PV power plant was used. The operating principle is such that when the voltage is too low, all the output power of the PV power plant is fed to the network. When the voltage is within the prescribed limits, all the output power of the PV power plant is used for charging the BESS. It is assumed that the BESS is half charged from the previous day. If the PV power plant alone cannot provide a suitable voltage profile, then the BESS is discharged as necessary to provide a suitable voltage profile. It was calculated that a BESS with a minimum nominal capacity of 30 kWh at a nominal power of 11 kW is needed to provide a suitable voltage profile in combination with the PV power plant. The output power profile of the PV power plant is shown in Figure 11. Figure 13 shows the SOC, charging and discharging power of the BESS at node 35. Figure 14 shows the voltage profile over time and nodes with a PV power plant and the BESS at node 35. In the discussed case, a suitable voltage profile is provided.

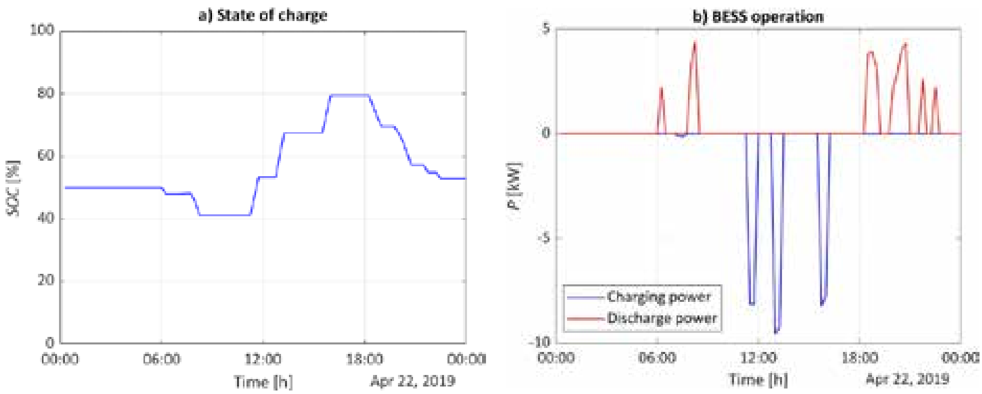

Figure 13: *SOC (a) and operation of BESS (b) at node 35 over time in combination with PV power plant*

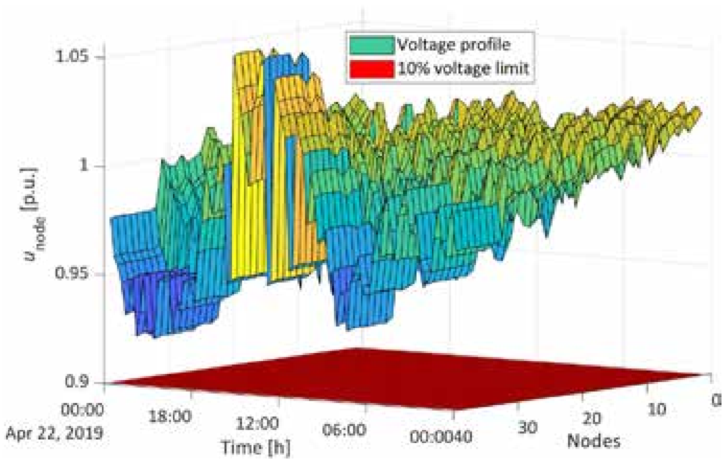

Figure 14: *Voltage profile over time and nodes with PV power plant and BESS at node 35*

5.2.6 Use of network users' energy flexibility service

At critical moments of the day, when the voltage was out of tolerance, we reduced and shifted consumption using the network users' energy flexibility service. The consumption was adjusted in a certain time interval, which lasted from 12:00 to 20:00, since in this interval there is the highest consumption. Consumers in the third feeder of the TS, where voltage profile violation occurred, were included in the flexibility service. There are five consumers with an installed power of 17 kW and one consumer with an installed power of 5 kW. Figure 15 shows the consumption profile using the flexibility service provided by the consumers with an installed power of 17 kW and 5 kW. Figure 16 shows the voltage profile using the flexibility service over an eight-hour time interval. Figure 16 shows that a suitable voltage profile is provided in this time interval.

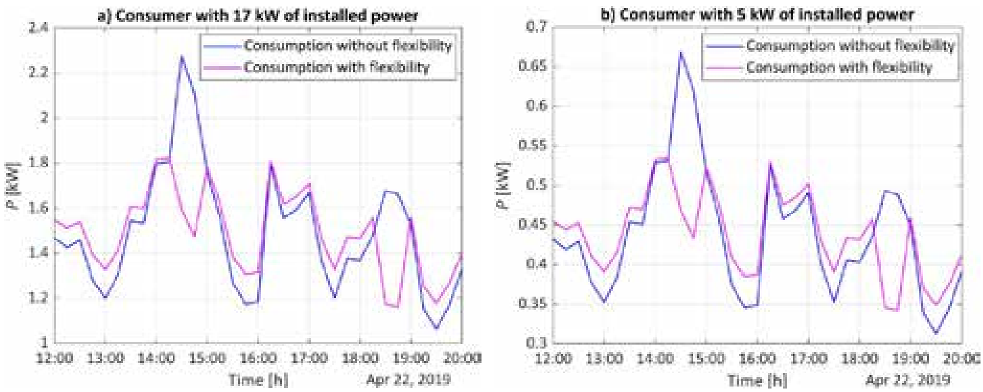

Figure 15: *Consumption profile over time using the flexibility service for consumer with an installed power of a) 17 kW, and b) 5 kW*

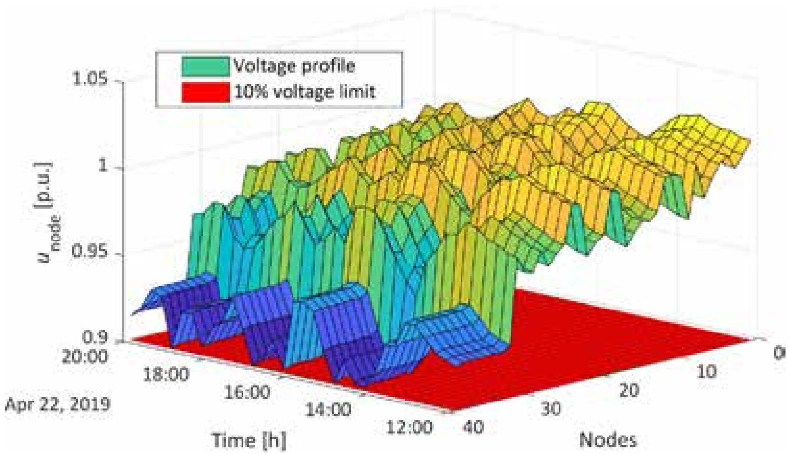

Figure 16: *Voltage profile using the flexibility service of consumers in third output of the TS*

5.2.7 Replacing network elements

The last solution to provide a suitable voltage profile is the replacement of network elements. It was assumed that the existing conductors would be replaced with conductors of a larger cross section in certain sections of the network in the third feeder of the TS. A larger conductor cross-section has a positive effect on the voltage profile and at the same time reduces losses in the network. In Figure 1, the feeder sections selected for the replacement of conductors are marked in green. These three sections were selected for replacement, because these are the longer lines in the third feeder with a smaller cross section of only 35 mm^2. All other lines in this feeder have a cross section of 70 mm^2. The existing conductors of type PP00-A 4x35+2.5 (cross section of 35 mm^2) were replaced with conductors of type PP00-A 4x70+2.5, which have a cross section of 70 mm^2. Conductors were replaced gradually in the three selected sectors. Figure 17 shows the voltage profile using a PP00-A 4x70+2.5 type conductor. A suitable voltage profile is provided when conductors in all three sectors are replaced.

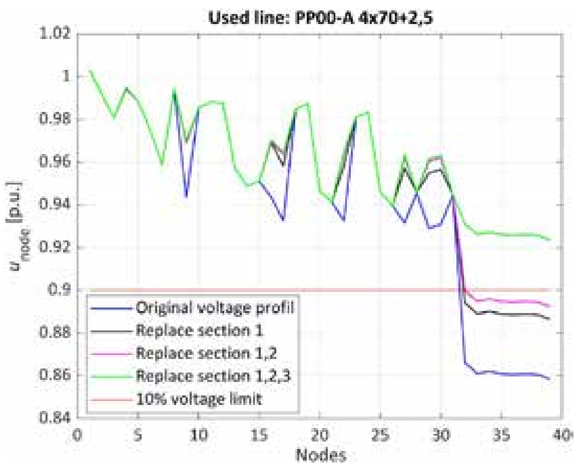

Figure 17: *Voltage profile with conductor type PP00-A 4x70+2.5 in selected sectors*

6 CONCLUSION

This article presents the results of the transformer overload analysis and the provision of suitable voltage profiles. The results were determined using load flow calculations. Calculations to provide a suitable voltage profile were performed for a symmetrical three-phase load using the BFS load flow method.

Transformer overload can be prevented by using a BESS of appropriate nominal capacity and power. With the network users' energy flexibility service, it is not possible to prevent overloading during the selected time interval. A longer time interval could be used, but this would shift the consumption to night-time hours, which does not make sense from the consumers' point of view.

A suitable voltage profile can be provided with a transformer with OLTC, where the voltage on the secondary side of the TR is increased. With a BESS of appropriate nominal capacity and power, a suitable voltage profile is provided. A combination of a BESS and a PV power plant can provide a suitable voltage profile. With the use of the network users' energy flexibility service, a suitable voltage profile is provided in the selected time interval. These results were obtained considering that all consumers in the third feeder of the TS participate, where the voltage profile violation occurred. By replacing the existing conductors with conductors of a larger cross-section in problematic sections, a suitable voltage profile is provided. A suitable voltage profile cannot be provided when reactive power compensation and a PV power plant are used as active network elements.

References

[1] **E. Bompard, E. Carpaneto, G. Chicco, R. Napol:** Convergence of the backward/forward sweep method for the load-flow analysis of radial distribution systems, International Journal of Electrical Power & Energy Systems, Volume 22, Issue 7, pp. 521−530, 2000

[2] **K. Prakash, A. Lallu, F. R. Islam, K. A. Mamun**: Review of Power System Distribution Network Architecture, 2016 3rd Asia-Pacific World Congress on Computer Science and Engineering, Suva, pp. 124-128, DOI:10.1109/APWC-on-CSE.2016.030, 2016

[3] **M. Sojer**: Voltage Regulating Distribution Transformers as new Grid Asset, Procedia Engineering, Volume 202, pp. 109-120, DOI: 10.1016/j.proeng.2017.09.698, 2017

[4] **P. S. Subramanyam**: Reactive Power Compensation, HOD, EEE Dept, for Internal Presentation in EEE Association, VBIT, Hyderabad, DOI: 10.13140/RG.2.2.20167.93602, 2019

[5] **J. Dixon, L. Moran, J. Rodriguez, R. Domke**: Reactive Power Compensation Technologies: State-of-the-Art Review, in Proceedings of the IEEE, vol. 93, no. 12, pp. 2144-2164, DOI: 10.1109/JPROC.2005.859937, 2005

[6] **C. K. Das, O. Bass, G. Kothapalli, T. S. Mahmoud, D. Habibi**: Overview of energy storage systems in distribution networks: Placement, sizing, operation, and power quality, Renewable and Sustainable Energy Reviews, Volume 91, pp. 1205-1230, DOI: 10.1016/j.rser.2018.03.068, 2018

[7] **K.C. Divya, J. Østergaard**: Battery energy storage technology for power systems—An overview, Electric Power Systems Research, Volume 79, Issue 4, pp. 511-520, DOI: 10.1016/j.epsr.2008.09.017, 2009

[8] **M. F. Akorede, H. Hizam, E. Pouresmaeil**: Distributed energy resources and benefits to the environment, Renewable and Sustainable Energy Reviews, Volume 14, Issue 2, pp. 724-734, DOI: 10.1016/j.rser.2009.10.025, 2010

[9] **A. Asrari, T. Wu, S. Lotfifard**: The Impacts of Distributed Energy Sources on Distribution Network Reconfiguration, IEEE Transactions on Energy Conversion, vol. 31, no. 2, pp. 606-613, DOI: 10.1109/TEC.2015.2514191, 2016

[10] **N. D. Hatziargyriou, A. P. Sakis Meliopoulos**: Distributed energy sources: technical challenges, 2002 IEEE Power Engineering Society Winter Meeting. Conference Proceedings (Cat. No.02CH37309), pp. 1017-1022 vol.2, DOI: 10.1109/PESW.2002.985163, 2002

[11] **M. van den Berge, M. Broekmans, B. Derksen, A. Papanikolaou, C. Malavazos**: Flexibility provision in the Smart Grid era using USEF and OS4ES, 2016 IEEE International Energy Conference (ENERGYCON), pp. 1-6, DOI: 10.1109/ENERGYCON.2016.7514067, 2016

[12] **Uredba o samooskrbi z električno energijo iz obnovljivih virov energije (Uradni list RS, št. 43/22), (en. Decree on the self-supply of electricity from renewable energy sources)**, 9.4.2022. Available: http://www.pisrs.si/Pis.web/pregledPredpisa?id=URED8432# (20.9.2022)

Nomenclature

BESS	Battery energy storage system
BFS	Backward-forward sweep
DER	Distributed energy resources
ESS	Energy storage system
LV	Low voltage
OLTC	On-load tap-changer
P	Active power
PV	Photovoltaic
Q	Reactive power
S	Apparent power
SOC	State of charge
t	Time
TS	Transformer station
u_{node}	Node voltage
U_{n}	Nominal voltage

Journal of Energy Technology

JET Volume 15 (2022) p.p. 53-64
Issue 3, 2022
Type of article: 1.01
www.fe.um.si/si/jet.html

RFCS PROJECT METHENERGY+ METHANE RECOVERY AND HARNESSING FOR ENERGY AND CHEMICAL USES AT COAL MINE SITES

RFCS PROJEKT METHENERGY+ ZAJEM METANA IN NJEGOVA ENERGETSKA TER KEMIČNA IZRABA V PREMOGOVNIŠTVU

Matjaž Kamenik[1R], Janez Rošer[1], Salvador Ordonez[2]

Keywords: ventilation air methane, abandoned mine methane, coalmining, methane recovery and harnessing, thermal or chemical upgrading, adsorption-based technologies, materials development, thermal and catalytic regenerative oxidizers, methanol, greenhouse gases.

Abstract

Ventilation Air Methane emissions (VAM) from coal mines lead to environmental concern because of their high global warming potential and the loss of methane (CH_4) resources. How to tackle methane harnessing and its use was studied and analysed in the scope of the RCFS project, which was performed from 2017 till 2020, and coordinated by the University of Oviedo in Spain within the scope of an international consortium of eleven entities from Poland, Spain, the United Kingdom, Czechia, Greece, Slovenia and Sweden, combining universities, research institutions and industry (mostly Polish mines and the Slovenian Velenje mine). The main challenge tackled

R Corresponding author: Dr. Matjaž Kamenik, Tel.: +386 3 899 6145, Mailing address: Premogovnik Velenje d.o.o., Partizanska cesta 78, 3320 Velenje. E-mail address: matjaz.kamenik@rlv.si.

[1] Premogovnik Velenje d.o.o., Partizanska cesta 78, 3320 Velenje

[2] Dep. of Chemical and Environmental Engineering (CRC), C. San Francisco, 3, 33003 Oviedo, Asturias, Spain

in the project was the use of methane released from both operating and abandoned mines, which is an environmental and safety hazard and also a useful source of energy. Therefore, the effective extraction of methane, its enrichment, purification, separation, thermal or chemical upgrading, and its use, considering coal mine site specifics, was assessed. Despite good operational results, after in-depth economic analysis of the integration, CAPEX and OPEX calculation, there turned out to be a high economic dependence on the cost of adsorbent, since adsorption was the most promising technology for concentrating the methane in these emissions. Therefore, the economic viability depends on the development of materials that meet a minimum cost and performance. Within the scope of the project, a lot of activities were carried out in order to widen and exploit the results.

Povzetek

Emisije odzračenega metana iz premogovnikov (t.i. VAM) imajo vpliv na okolje zaradi visokega toplogrednega učinka metana, po drugi strani pa pomenijo izgubo energetskega vira. Kako in na kakšen način izkoristiti metan, je bilo preučeno in analizirano v okviru RCFS projekta, ki se je izvajal od leta 2017 do leta 2020. Koordinator projekta je bila Univerza v Oviedo iz Španije, projektni mednarodni konzorcij pa je sestavljalo enajst partnerjev iz Poljske, Španije, Združenega kraljestva, Češke, Grčije, Slovenije in Švedske. Konzorcij je združeval univerze, raziskovalne ustanove in industrijo (večinoma Poljske premogovnike in Slovenski Premogovnik Velenje). Glavni izziv projekta je bila preučitev možnosti zajema in uporabe metana, emitiranega iz delujočih in zaprtih premogovnikov, saj je le-ta škodljiv za okolje in predstavlja varnostno tveganje, po drugi strani pa koristen energetski vir. Vsled tega se je preučila učinkovita ekstrakcija metana, njegova obogatitev, očiščenje, separacija, toplotna ali kemična nadgradnja in njegova uporaba ob upoštevanju specifik posameznih premogovnikov. Kljub dobrim operativnim rezultatom, poglobljeni ekonomski analizi integracije, izračunom investicijskih in obratovalnih stroškov, se je pokazala velika odvisnost ekonomike od stroškov adsorbenta, saj je bila adsorpcija najbolj obetavna tehnologija za koncentracijo metana glede na velikost emisij. Zaradi tega je ekonomska opravičenost pogojena z razvojem materialov, ki bodo imeli nizke stroške in istočasno dobro učinkovitost. V okviru projekta se je opravilo veliko aktivnosti z namenom razširjanja in eksploatacije rezultatov.

1 INTRODUCTION

Coal mine Premogovnik Velenje (PV) participated in the EU's METHENERGY+ project, cofounded by the Research Fund for Coal and Steel (RFCS) programme. RFCS is an EU funding programme supporting research projects in the coal and steel sectors. The RFCS has its own legal basis and stands outside the Multiannual Financial Framework. It is funded via the revenues generated by the European Coal and Steel Community (ECSC) in liquidation assets, which are exclusively devoted to research in the sectors related to the coal and steel industries.

The project with title and subject "Methane recovery and harnessing for energy and chemical uses at coal mine sites", was performed from 2017 till 2020, and was coordinated by the University of Oviedo in Spain within the scope of an international consortium of eleven entities from Poland, Spain, the United Kingdom, Czechia, Greece, Slovenia and Sweden, combining universities, research institutions and industry (mostly Polish mines and the Slovenian Velenje mine).

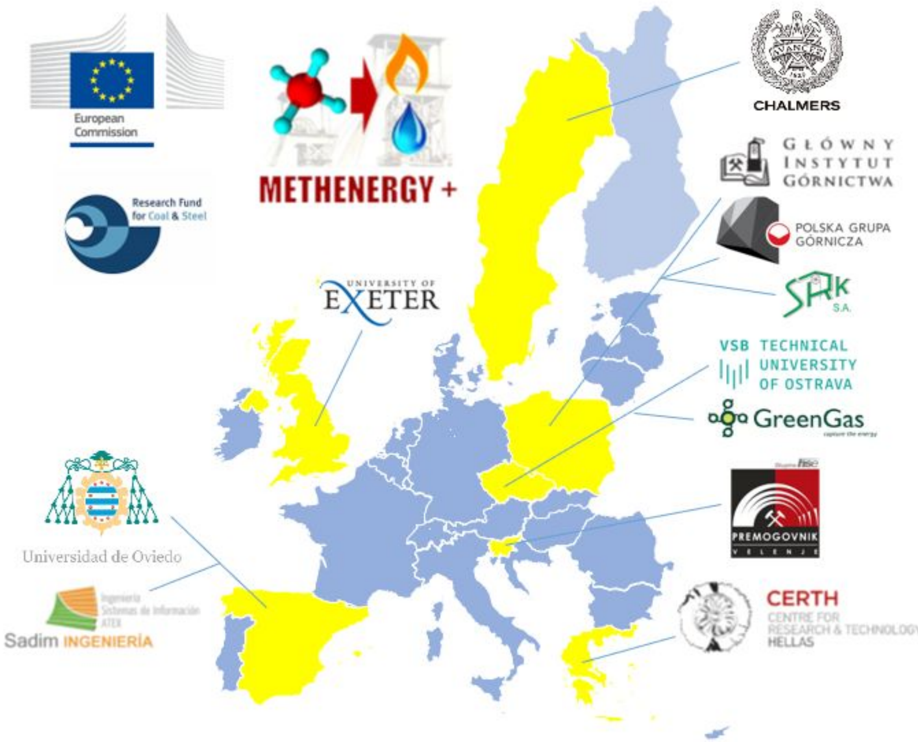

Figure 1: *Project METHENERGY+ partners*

The main challenge tackled in project was the use of methane released from both operating and abandoned mines, which is an environmental and safety hazard and also a useful source of energy and raw material for manufacturing chemicals. Therefore, effective methane extraction, its enrichment, purification, separation, thermal or chemical upgrading, and its use, considering coal mine site specifics, was assessed.

2 SOURCE OF METHANE

Coal production releases CH_4 trapped in coal seams and surrounding strata, and which can be categorised into three types:

- CH_4 drained from the seam before mining (60–95% CH_4),
- CH_4 drained from worked areas of the mine (30–95% CH_4), and
- CH_4 diluted through ventilation fans (0.1–1.5% CH_4) while extracting coal.

Therefore, there are mainly three different types of mining emissions containing methane:

- coal bed methane (CBM),
- abandoned mine methane (AMM) and

- ventilation air methane (VAM).

The first two usually contain high and medium purity methane (>30%), and are easily exploited with the well-known harnessing technologies available.

VAM has a very low concentration, so it has very low energy efficiency, and is in most cases vented into the atmosphere via underground coal mine fan stations.

In the case of Premogovnik Velenje in Slovenia, the maximum allowed gas concentration at fan stations is 0.5%, which is carefully monitored due to safety reasons. What also needs to be highlighted are the widely fluctuating concentrations resulted from underground mining activities. Major influence factors include the intensity of mine face production and also mining method, mine geology and type of coal extracted. In the project, concentrations and parameters from partner mines where average VAM concentrations in the range 0.1–0.3% CH_4 with very high total flow rates (even as high as 200 Nm^3/s) were considered.

Therefore, based on the average results of several authors and measured concentrations in project partner mines, a stream with fair to moderate methane concentration and air flow rate values has been selected for the analysis made: 0.57% CH_4 and 4.4 Nm^3/s, respectively [2].

3 SCOPE OF THE PROJECT

The scope of the project was:

1) Optimisation of methane recovery (methane concentration and flow rate) at operating and flooded coal mines, considering the geological and operational features of the shafts.

2) Development of adsorption-based technologies for concentrating methane from ventilation air methane (VAM) and abandoned mine methane (AMM) emissions, including materials development and process design and simulation. Different approaches will be used for preparing the potential adsorbents, including the development of high-performance tailored materials or the use of waste materials from other processes as adsorbents.

3) Development of a membrane-based technology for the separation of methane from VAM and AMM emissions, including the development of perm-selective membranes using nano-structured materials, as well as the modelling and simulation of these units at industrial scale.

4) Explore the possibility of using thermal and catalytic regenerative oxidizers for the efficient and environmentally safe combustion of these emissions (with and without previous methane enrichment).

5) Explore the possibility of transforming the methane contained in the studied emissions (with or without further enrichment) into other valuable chemicals, such as methanol or hydrogen.

6) Evaluate the application of the above technologies for methane enrichment and utilisation, both to operating mines and to mines where coal mining activity has ceased.

3.1 Methane recovery at deep coal mine sites within the whole life cycle of a mine

Exhaustive research and analytical work was carried out to demonstrate the impact of various factors on the possibility of collecting and flowing water and methane in mining excavations, with particular emphasis on mine closure. On the basis of a review of the methods of capacity assessment of underground water reservoirs and filtration properties in the rock mass, using the methods of mining hydrogeology, a description of the process of water and gas accumulation and the conditions of their flow in mining excavations and in goafs was prepared. A database was prepared on selected components of mine gases for 15 active and 1 closed mine, with a total of 32 shafts in the analysis. The results of measurements of methane concentration, temperature, humidity and air composition for all available levels were presented. A total of approximately 50,000 datapoints were compiled and analysed. Moreover, a catalogue of the main natural and technical factors determining the flow and accumulation of methane and water in the workings of active and liquidated mines was developed. An outline of the recommended methodology for estimating the amount of gas (methane) emitted during the flooding of mining excavations is presented in the example of a liquidated test mine. The geological, mining and hydrogeological conditions and the impact of their changes on the methane potential of the mines on the scale of the coal basin were verified. The impact of these conditions on the possibility of considering scenarios and models of mine closure in terms of methane recovery was assessed. Further development of the scenarios was carried out.

3.2 Adsorption technologies for methane recovery in VAM

Research work was done on adsorption technologies for methane recovery in VAM to establish the potential of adsorption processes for the separation of methane from ventilation gases, to gather relevant data on the most appropriate adsorbents and adsorption technologies, depending on the characteristics of the emissions, and to model on the lab scale in order to provide useful information for implementation at the mine site. More materials were considered and compared, including porous carbon materials from zeolite, zeolites prepared from fly-ashes, and MOFs[1] (two different families, Basolites and IRMOFs). Adsorption processes were rigorously modelled, both taking into account adsorption and desorption steps. Modelling codes were experimentally validated for different materials considered in this project. A process based on the use of temperature swing adsorption (TSA) was proposed and designed.

3.3 Tailored materials for methane recovery using membrane processes

Tailored materials for methane recovery using membrane processes were assessed and studied to:

- establish the potential for the separation of methane from ventilation gases using membrane technologies
- determine the optimum materials and procedures for the preparation of membranes for methane concentration in VAM

[1] Metal-Organic Framework.

- To model the lab scale results in order to provide useful information for implementation at mine sites

Mass transfer has been modelled using the Maxwell-Stefan multicomponent surface diffusion model. The model performance has been validated using the limited literature data available for this type of mixture. The application of this model has been extended by simulating the concentration profiles along the length of the membrane module using the plug flow model.

3.4 Combustion technologies

There was a systematic comparison of thermal (TFRR or RTO) and catalytic (CFRR or RCO) flow reversal reactors for methane abatement in mine gases. Attention was also devoted to designing a reactor for mine implementation in order to reduce VAM and AMM emissions and to optimise the design of control strategies for this kind of reactor. Formation of secondary pollutants (NOx), which are present especially in the case of CFRR, was determined.

Methane concentration in ventilation air of the different mines analysed ranges from 0.10% to 0.25% (vol.) in most situations. These are very low values, which can be handled by RCO (minimum concentration of 0.18%), but barely with RTO (minimum concentration of 0.36%). In the latter case, only the use of high efficiency regenerative oxidizers may lead to autothermal operation, e.g. for a methane concentration of 0.25% the thermal efficiency should be higher than 93%.

Environmental and safety issues associated with these technologies were deeply analysed. Secondary environmental impacts of these technologies are negligible. Concerning safety constraints, these are also manageable.

The recovery of the energy associated with methane from coal mine ventilation air emissions can be done using lean-burn gas turbines (EDL, CSIRO, IR, etc.). These types of turbine are especially suited to work with low methane concentrations and are able to produce work (electricity) directly. Lean-burn turbines are not widely used for the harnessing of VAM, because they require a minimum methane concentration of 1% [7], which is rather high for most VAM emissions. Hence, a prior methane concentration step is needed. A combination of adsorption processes with gas turbines has been proposed in this work as a realistic strategy for upgrading these emissions.

3.5 Chemical upgrading of VAM

The objectives of this work package were the following:

To select catalytic technologies for the conversion of methane at the conditions encountered both in mine methane emissions and in methane-enriched emissions.

To select and test under real conditions the catalysts and reactors useful for methane upgrading in mine methane emissions.

To study the influence of reactor configurations and operating variables on the performance of the system.

The most promising upgrading approach for both enriched VAM and AMM are based on the direct oxidation to methanol. Among the different approaches suggested in the literature, gas phase heterogeneous oxidation using metal loaded zeolites seems to be the most feasible alternative.

Different Cu and Fe-loaded zeolites were prepared and tested for the direct oxidation of methane, the best results being obtained with Cu-loaded mordenite.

A preliminary design of a process based on this approach has been accomplished. The upgrading of diluted methane emissions into valuable products can be accomplished at low temperatures (200°C) by the direct partial oxidation of methanol over copper-exchanged zeolite catalysts. The reaction has been studied in a continuous fixed-bed reactor loaded with a Cu−mordenite catalyst, according to a three-step cyclic process: adsorption of methane, desorption of methanol, and reactivation of the catalyst. The purpose of the work is the use of methane emissions as feedstocks, which is challenging due to their low methane concentration and the presence of oxygen. Methane concentration had a marked influence on methane adsorption and methanol production (decreased from 164 μmol/g Cu for pure methane to 19 μmol/g Cu for 5% methane). The presence of oxygen, even in low concentrations (2.5%), reduced methane adsorption drastically. However, methanol production was only affected slightly (average decrease of 9%), concluding that methane adsorbed on the active centres yielding methanol is not influenced by oxygen [4].

It has been demonstrated that the desired reaction can be accomplished even in the presence of air. For this purpose a cyclic operation was proposed, treating the catalyst with the methane containing gas and with steam in successive cycles. These cycles have been optimised during this period.

Evaluation and integration

A methodological approach for determining methane recovery from both operating and abandoned coal mines has been developed. The approach takes into account hydrogeological modelling of the coal basins.

Integrated processes for the harnessing of coal mine ventilation air methane has been proposed, designed and economically evaluated. The concentration of methane in the ventilation air is a critical parameter for the selection and design of an adequate harnessing technique. This concentration may differ from mine to mine, and at different times during mine operation. However, during the mine closure and flooding processes, this concentration may increase for some mines. The mine case study considered a ventilation air flow rate of 4.41 Nm^3/s with methane concentration of 0.57%.

The use of a prior concentration stage based on fixed-bed adsorption has been proposed to raise methane concentration before harnessing. In this context, two integrated schemes have been analysed and proposed:

Adsorption + Combustion in regenerative oxidizer. The fixed-bed adsorption unit is filled with Norit GF-40 active carbon as adsorbent. For this concentration, heat recovery efficiency can be as high as 54%, which corresponds to an equivalent saving of 36.5 Nm^3/h of natural gas.

Adsorption + Combustion in a gas turbine. In this case, the ventilation air is concentrated in a fixed bed equipped with Basolite C300 adsorbent. This adsorbent is capable of concentrating methane from 0.57% to 1.2%. The resulting concentrated stream is harnessed in a gas turbine with a generation of 490 kW of net power as electricity.

Next we describe case 2, where the concentration step is carried out in a fixed bed temperature-swing adsorption (TSA) operation. This unit is inherently discontinuous, with adsorption happening in the first step and, once the adsorbent is saturated, methane is recovered by desorption at a higher temperature. The concentration step must increase methane concentration to a minimum of 1% in order to use a lean-burn gas turbine for the combustion.

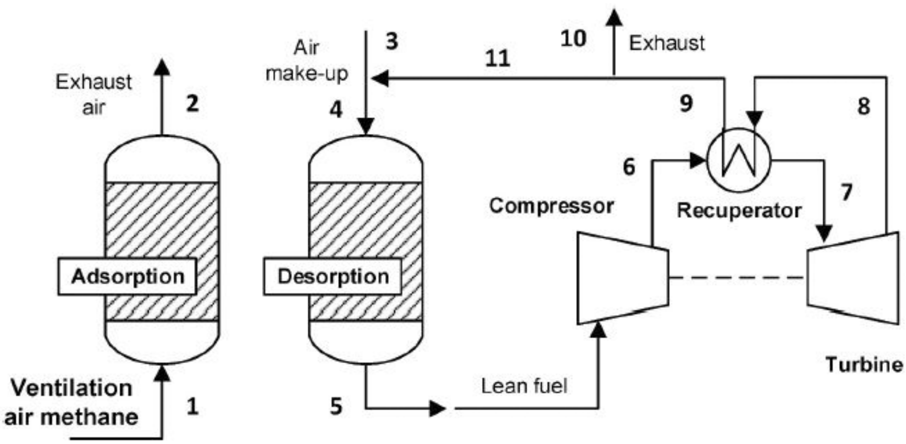

Figure 2: *Flowsheet of the TSA-turbine integrated process.*

The lean-burn gas turbine is made of three elements: compressor, recuperator and turbine. The turbine is capable of generating net work and, hence, produce electricity. The recuperator is used to pre-heat the feed before combustion using part of the energy of the combustion gases. In addition, part of these combustion gases can be used as the drag stream of the desorption process as shown in upper Figure [5]. This level of mass and heat integration is critical in order to save energy and improve the economy of the process.

4 ECONOMIC EVALUATION

The next economic evaluation shown is for adsorption and combustion in a gas turbine case, as described in the previous section.

The process is mass and energy integrated, since the heat required by the adsorption/desorption operation is fully supplied by the exhaust from the gas turbine.

The entire design includes the material and devices needed to carry out the whole project. The economic evaluation has been done using the guidelines provided by the US Environmental Protection Agency (EPA). This organisation has published a document entitled “Air Pollution Control Cost Manual” [6], which provides guidance for the design and costing of the equipment used for pollution control.

Table 1: *The capital investments–Adsorption and combustion in a gas turbine*

CAPITAL INVESTMENT		
Direct Costs		
Purchase equipment costs		
Equipment cost	A	2 313 031 €
Instrumentation	0.1A	231 303 €
Sales taxes	0.03A	69 391 €
Freight	0.05A	115 652 €
Total	B=1.18A	2 729 377 €
Direct installation costs		
Foundations & supports	0.08B	218 350 €
Handling & erection	0.14B	382 113 €
Electrical	0.04B	109 175 €
Piping	0.02B	54 588 €
Insulation for ductwork	0.01B	27 294 €
Painting	0.01B	27 294 €
Total	0.3B	818 813 €
Total Direct Costs	DC=1.3B	3 548 190 €
Indirect Costs		
Engineering	0.10B	272 938 €
Construction	0.05B	136 469 €
Contractor fees	0.10B	272 938 €
Start-up	0.02B	54 588 €
Performance test	0.01B	27 294 €
Total Indirect Costs	IC=0.28B	764 226 €
Contingency costs	CC=0.10(DC+IC)	431 242 €
Total Capital Investment	**TCI=DC+IC+CC**	**4 743 657 €**

The Main Equipment Costs exclude the piping, instrumentation and auxiliary equipment. These costs are accounted for as direct costs of the Capital Investment, which are estimated as a function of the total Cost of Main Equipment (Cost reports and guidance, 2018). Final calculated Total Capital Investment (TCI) is 4.74M €.

The Annual Operating Costs have also been estimated.

Table 2: *Annual operating costs of the integrated adsorption and gas turbine*

Annual operating costs of the integrated adsorption and gas turbine.

ANNUAL OPERATING COSTS		
Direct Annual Cost	8000 h/year	
Operating Labour		
Operator	0.5 h/shift	12 925 €
Supervisor	15% operator	1 939 €
Operating Materials	-	
Maintenance		
Labour	0.5 h/shift	13 191 €
Materials	100% labour	13 191 €
Adsorbent replacement		6 972 687 €
Utilities		
Electricity consumed	0.07€/kWh	16 324 €
Electricity generated	0.07€/kWh	-274 288 €
Total Direct Annual Costs		6 755 968 €
Indirect Annual Cost		
Overhead	60% op. maint.	24 747 €
Administrative charges	2% TCI	94 873 €
Property taxes	1% TCI	47 437 €
Insurance	1% TCI	47 437 €
Capital recovery		-167 623 €
Total Indirect Annual Cost		46 870 €
Total Annual Cost		**6 802 838 €**

These costs include labour, materials, maintenance, utilities and administrative charges. A yearly operation of the plant of 8,000 hours has been considered in the calculations. Additionally, the necessary replacement of the adsorbent used should also be considered as Annual Operating Cost, since these materials have a lifetime that is lower than that of the main equipment, such as vessels or fans. It has to be replaced periodically due to degradation and loss of capacity. For this reason, its cost must be divided and accounted for as annual, following the recommendations of the EPA, considering a lifetime of n = 4 years and an interest rate of i = 4.25%, which results in a factor FWF = 0.2346. An additional 8% is added to account for freight and taxes. The cost of the adsorbent is a key parameter in the economic study, so a sensitivity analysis was performed in order to study the viability of the process depending on it. From now on, an arbitrary X value is considered for the cost of 1 kg of adsorbent material.

The utilities consist electricity consumed by the fan, which provides the required gas flow rate through the different equipment. Considering an electricity price of 0.07 €/kWh and the power consumption of the fan (147 kW), the annual electricity consumption cost is estimated at 82,320 €/year. However, the gas turbine is able to generate 490 kW of net work, directly as electricity. This power should be discounted from that consumed by the process. Considering the same electricity price, the gas turbine generates earnings of 274,288 €/year, which are included as negative costs in Table 2. As shown, the total annual cost depends heavily on the adsorbent material cost

(X). In addition to the costs reflected in previous tables, the positive environmental impact of the process should be taken into account. This is accounted for by the carbon emission allowances.

The economic evaluation points out the importance of the adsorbent cost. In fact, for the process to become profitable, a lower adsorbent cost of 0.6 €/kg is desirable.

Results of the economic evaluation for different adsorbent costs (X). Annual cash flow (blue line), NPV (orange line). Black arrows point out the necessary adsorbent cost to make the NPV equal to zero.

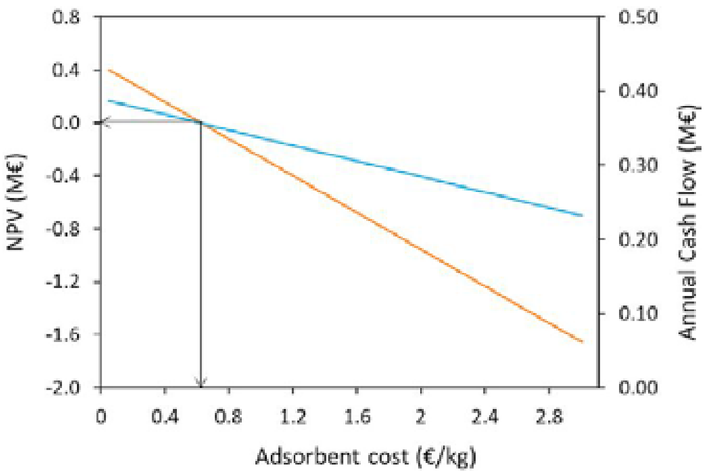

Figure 3: *Economic evaluation at different adsorbent costs*

Therefore, the final conclusion is that the technical feasibility of both combinations has been demonstrated, whereas the economic viability will depend on the development of materials that meet a minimum of cost and performance.

5 CONCLUSIONS

As there were several mining companies involved, different technical solutions were offered depending on the characteristics of each mine site. Among the studied approaches, the combination of an adsorption process and a gas turbine seems to be the most attractive approach for future implementation. This project proposes the combination of three strategies for solving this significant problem:

1) Optimise the ventilation procedures in order to get the highest CH_4 concentrations extractable under safe conditions. This activity has been extended to abandoned and flooded mines, for which higher methane concentration can be achieved.

2) The development of procedures for concentrating the methane in these emissions. The most promising technologies are those based on adsorption and membrane technologies.

3) Study of combustion and chemical transformation technologies in the presence of oxygen. In previous research, it has been observed that flow reversal combustors provide the best performance for the combustion of these emissions, but there remain several underexplored aspects,

such as the environmental effects, the control strategies, and integration with the overall energy management system of the plant.

This work has studied the feasibility of harnessing low-concentrated methane streams by integrating two independent processes: temperature swing adsorption for methane concentration, followed by combustion in a lean-fuel burn turbine for obtaining a surplus of electricity and calorific energy. The design has been made for a VAM inlet stream, which has a flow rate of 4.4 m^3/s, with an average methane concentration of 0.57% CH_4 in air.

Despite the good operational results, after in-depth economic analysis of the integration the process shows a high dependence on the cost of adsorbent.

A lot of activities were carried out in order to widen and exploit the results. It should be noted that an important part of the results was published. Regarding the industrial exploitation of the results, the deep study about methane release during mine operation and flooding will be very helpful for designing ventilation systems. For example, the next fan stations and ventilations systems planned for underground mines in the future could be done in reference to the findings of this project.

Project METHENERGY+ has been proposed as an example of global warming related initiatives performed at the University of Oviedo within the activities heldin Oviedo. Project was presented at several conferences in Spain, Germany and Poland.

References

[1] **METHENERGY+.** Universidad de Oviedo. Project reports and website. http://www.unioviedo.es/METHENERGY/, 2022

[2] **David Ursueguía, Pablo Marín, Eva Díaz, Salvador Ordonez:** *A new strategy for upgrading ventilation air methane emissions combining adsorption and combustion in a lean-gas turbine*, Journal of Natural Gas Science and Engineering, Journal of Natural Gas Science and Engineering 88 (2021) 103808

[3] **Ukrit Chaemwinyoo, Pablo Marín, Claudia Fern´andez Martín, Fernando V. Díez, Salvador Ordonez:** *Assessment of an integrated adsorption-regenerative catalytic oxidation process for the harnessing of lean methane emissions*, Journal of Environmental Chemical Engineering 10 (2022) 107013

[4] **Mauro Álvarez, Pablo Marín, and Salvador Ordóñez:** *Harnessing of Diluted Methane Emissions by Direct Partial Oxidation of Methane to Methanol over Cu/Mordenite,* Ind. Eng. Chem. Res. 2021, 60, 9409−9417

[5] **Su, S., Beath, A., Guo, H., Mallet, C.:** *An assessment of mine methane mitigation and utilisation technologies*. Prog. Energy Combust. Sci. 31, 123–170. https://doi.org/10.1016/j.pecs.2004.11.001, 2005

[6] **Cost reports and guidance**: https://www.epa.gov/economic-and-cost-analysis-air-pollution-regulations/cost-reports-and-guidance-air-pollution, 2018

[7] **Yin, J., Su, S., Yu, X., Weng, Y.:** *Thermodynamic characteristics of a low concentration methane catalytic combustion gas turbine*. Appl. Energy 87, 2102–2108. https://doi.org/10.1016/j.apenergy.2009.12.011. 2010

Journal of Energy Technology

JET Volume 15 (2022) p.p. 65-74
Issue 3, 2022
Type of article: 1.01
www.fe.um.si/si/jet.html

MEASUREMENT DEVICE FOR TESTING PRINTED CIRCUIT BOARD ASSEMBLIES COMING OFF THE PRODUCTION LINE

MERILNA NAPRAVA ZA PREIZKUŠANJE TISKANIH VEZIJ IZ PROIZVODNJE

Nejc Friškovec[1ℜ], Manja Obreza[1], Sebastijan Seme[1,2], Klemen Sredenšek[1]

Keywords: electrical measurement, printed circuit board, testing device, automation, intelligent measuring system

Abstract

The paper presents an efficient way to evaluate and determine the quality of an assembled printed circuit board coming off the production line. A printed circuit board assembly consists of electronic devices soldered to the printed circuit board, which provides the electrical connections. After assembling the printed circuit board, a function test needs to be performed to guarantee the quality of the product. Usually, the assembly lines are equipped with cameras that detect inaccuracies such as missing components. This level of quality assurance is sometimes not enough, and we need to add another degree of precaution. In addition to camera inspections, electronic measurements must be conducted. The process needs to be automated to provide repeatability and speed. The paper evaluates such a device and presents its advantages, disadvantages, and complexity. The device includes an electrical part that performs the measurements, a mechanical part that consists of a housing and a mounting nest, and a program that supervises the process.

ℜ Corresponding author: Nejc Friškovec, E-mail address: nejc.friskovec@student.um.si

[1] Faculty of Energy Technology, University of Maribor, Hočevarjev trg 1, Krško, Slovenia

[2] Faculty of Electrical Engineering and Computer Science, University of Maribor, Koroška cesta 46, Maribor, Slovenia

Povzetek

Raziskovalno delo predstavi efektiven način ocenjevanja in določanja kakovosti tiskanih vezij iz proizvodnih linij. Sestavljeno tiskano vezje zagotavlja električno povezavo prispojenim elektronskim komponentam. Po sestavi tiskanega vezja je potrebno izvesti funkcionalen preizkus, ki zagotavlja kakovost izdelka. Proizvodnje linije so ponavadi opremljene z inšpekcijskimi kamerami, ki odkrivajo nepravilnosti, kot so manjkajoče komponente. Vendar takšen način zagotavljanja kakovosti v nekaterih primerih ni zadosten, zato je potrebna dodatna raven nadzora. Poleg inšpekcij s kamerami je potrebno izvesti tudi električne meritve. Proces teh meritev mora biti avtomatiziran za zagotovljanje njegove ponovljivosti in hitrejše izvedbe. Raziskovalno delo ovrednoti pomen takšne naprave, predstavi njene prednosti in slabosti ter kompleksnost. Naprava obsega elektronski del, ki izvaja meritve, mehanski del, ki obsega ohišje in vpenjalno mesto, ter program, ki nadzira proces.

1 INTRODUCTION

Printed circuit boards (PCBs) have been a part of our lives for decades, facilitating everyday life as well as bringing more comfort. From an engineering point of view, PCBs make the construction and design of electronic projects easier, as they represent simple electronic connections *[1]*. Electric components are mounted on the PCB with through-hole technology (THT) or surface-mount devices (SMD), put together on advanced assembly lines that solder the desired component to the PCB through automation *[2]*. The assembly line consists of a loader that places the empty PCBs on the line, followed by the glue dispenser, which distributes the solder paste on the surface. The component placement machines place the electrical components on the PCB where the solder pads are located, and the last step consists of the reflow oven, where the components are soldered by hot air. The system is completed with the unloading of the assembled, cooled and camera-inspected PCBs *[3]*.

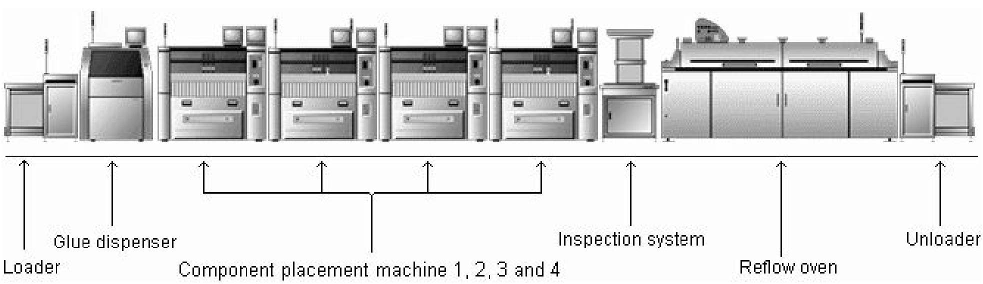

Figure 1: *Assembly line for PCBs [3]*

After assembly, the printed circuit board assembly (PCBA) could still have some errors, like damaged components or poor connections. Those inaccuracies could be detected with an intelligent measuring system *[4]*. That kind of device requires a procedure that can evaluate faults that occur while being assembled. So-called intelligent measuring systems come in the form of testing devices (TDs) that automate the measurement process. They need to measure all the required electrical components and quantities given by the developer of the tested circuit board. The TD needs to be designed with great care because it needs to be reliable and have a quick response time in order to minimise the cost of production. Such a device is extensive because it consists of a mechanical, an electrical, and a programming part of engineering. The electrical part must ensure that all the measurements can be acquired and that any additional damage is prevented in case of PCBA failure. The mechanical part must have a solid housing that provides all connection ports. Add-ons must include a mechanism that ensures an electrical connection with the measured PCBA. The programming part executes the automation of measurements with pre-written protocols.

The principle of all measurements is based on the fundamental laws of electrical engineering, such as Kirchoff's Current Law, which states that for any junction in an electrical circuit, the sum of currents flowing into that node is equal to the sum of currents flowing out of that node. It is often used with Ohm's Law to perform nodal analysis, which states that current through a conductor between two points is directly proportional to the voltage across the two points. Kirchoff's Voltage Law declares that the directed sum of potential differences or voltages around any closed loop is zero *[5]*. The voltage measurement in this project was performed using an analog-to-digital converter (ADC) with 12-bit resolution *[6]*. The results are represented as measurement errors describing the deviation of measured values to the actual values. As the name suggests, the random error is random and cannot be eliminated in practice. The system error can and must be eliminated from the measurement *[7]*.

2 MATERIALS AND METHODOLOGY

2.1 Protocol of measurements

The TD must satisfy all requirements that the developer of the circuit determines. In our case, two circuits need to be inspected, one with eleven and one with six requirements. The first PCBA has five different voltages applied with linear voltage regulators on the tested board. It has a microprocessor with wireless technology (Wi-fi) and Bluetooth that require evaluation. A long-range (LoRa) module is integrated into the PCBA and needs to be tested. Significant communication and control lines also need to be checked, such as a Universal Asynchronous Receiver-Transmitter (UART), Inter-Integrated Circuit (i2c) protocols, and the operation of the MOSFET transistor. The second PCBA consists of two different voltages that need to be measured, as well as the functionality of the microprocessor and LoRa module. In addition, a 24-bit ADC mounted on the PCBA needs to be examined. On both PCBAs, a program for further use needs to be uploaded.

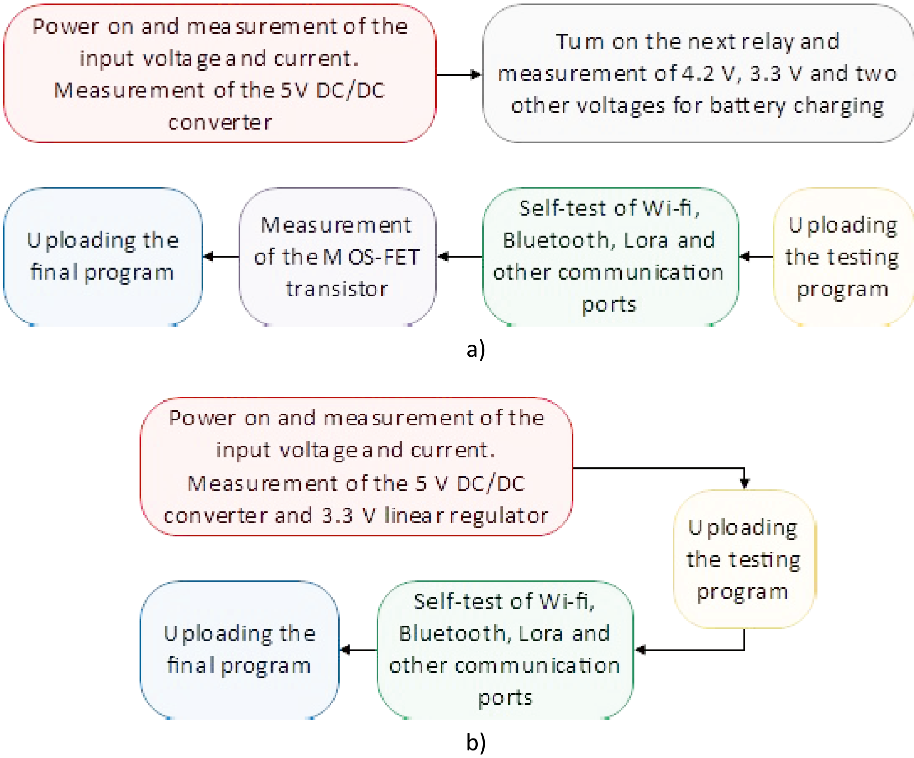

***Figure 2:** Protocol of measurements for the first (a) and second (b) PCBA*

2.2 The electrical part of the testing device

The fundamental parts of the TD are the power supplies. The device is powered by 230 V AC and consists of an alternating to direct current (AC/DC) power supply that powers the testing device, and separate AC/DC power supplies for the tested devices. Separate power supplies are mandatory because the testing device needs to stay in operation in case of a short circuit on the tested board. The heart of the testing device is an LX6 microprocessor (240 MHz) powered by 3.3 V and consists of a 12-bit ADC and 17 general-purpose input/output pins *[8]*. The processor can be programmed with C or C++ via Universal Serial Bus (USB) to Time To Live (TTL). The processor executes the measurements, evaluates them, and sends the results to a server. To complete the measurements, we need to provide an electrical connection from the testing device to the tested PCBA. Various contact probes are used to provide the connection, as shown in Figure 3. The model of the probe is selected based on the PCBA surface connection port. Usually, the developer of the tested board has already determined special pins that are only for testing purposes.

Figure 3: *Contact probes [9]*

2.3 The mechanical part of the testing device

The mechanical part consists of a housing and the mechanical clamping of the testing PCBA to the TD. The housing must be compact and provide the necessary connection ports and component mountings. Part of the top housing comprises the mechanical clamping, also known as the nest, consisting of AL4040 profiles where AMF clamps are mounted. The clamp pushes the tested PCBA into the nest, where the contact probes are located (Figure 4).

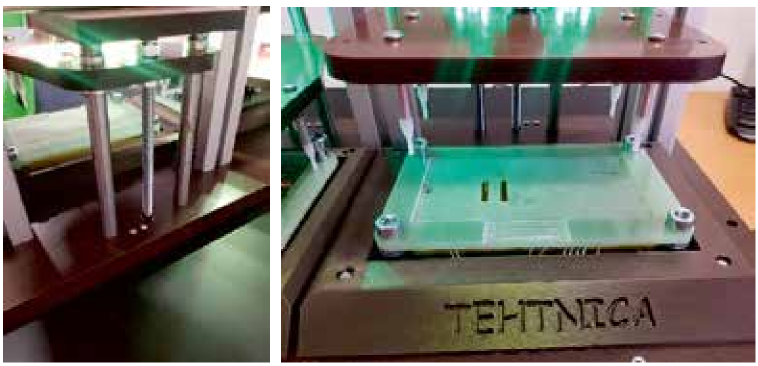

Figure 4: *Clamping mechanism*

The nest is protected by a 3-dimensional printed shield that protects the worker performing the measurements. The measurement starts when the clamp is fully pushed down, triggering a limit switch. The construction is shown in Figure 5.

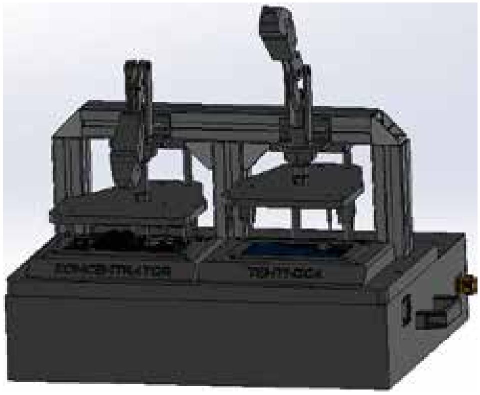

Figure 5: *The testing device*

2.4 Programming of the testing device

Programming of the microprocessor is done with the C++ programming language. The measured data is sent via USB to the server, and the TD functions with two processors, one for each nest and its program. Two additional programs were written and uploaded to the testing PCBAs, which carry out self-testing. The voltage is measured with the ADC with the help of resistor voltage dividers, whose characteristic is non-linear (shown in Figure 6). Therefore, the measurement can be solved using the characteristic transformation given by (1.1).

$$U_{real} = -1.6 \cdot 10^{-12} \cdot U^4 + 118.171 \cdot 10^{-12} \cdot U^3 - 301 \cdot 10^{-9} \cdot U^2 + 1.10902 \cdot 10^{-3} \cdot U + 0.034 \quad (1.1)$$

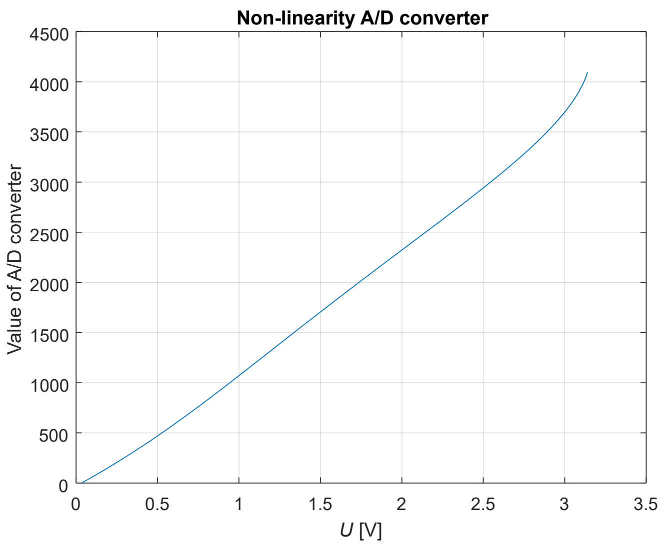

Figure 6: *Non-linearity of the ADC*

3 RESULTS

In the process of designing the testing device, we need to take into consideration the needs of production in the factory. The safety of workers and the provision of quality are the primary concerns. Safety is ensured with features such as 3D printed parts by the nest, low resistance grounding of the metal objects, and an emergency stop button. A functional test must be performed to provide quality measurements before every series. The functionality test is necessary to discover all the failures on the PCBA. Figure 7 presents all the possible failures and PCBAs with errors.

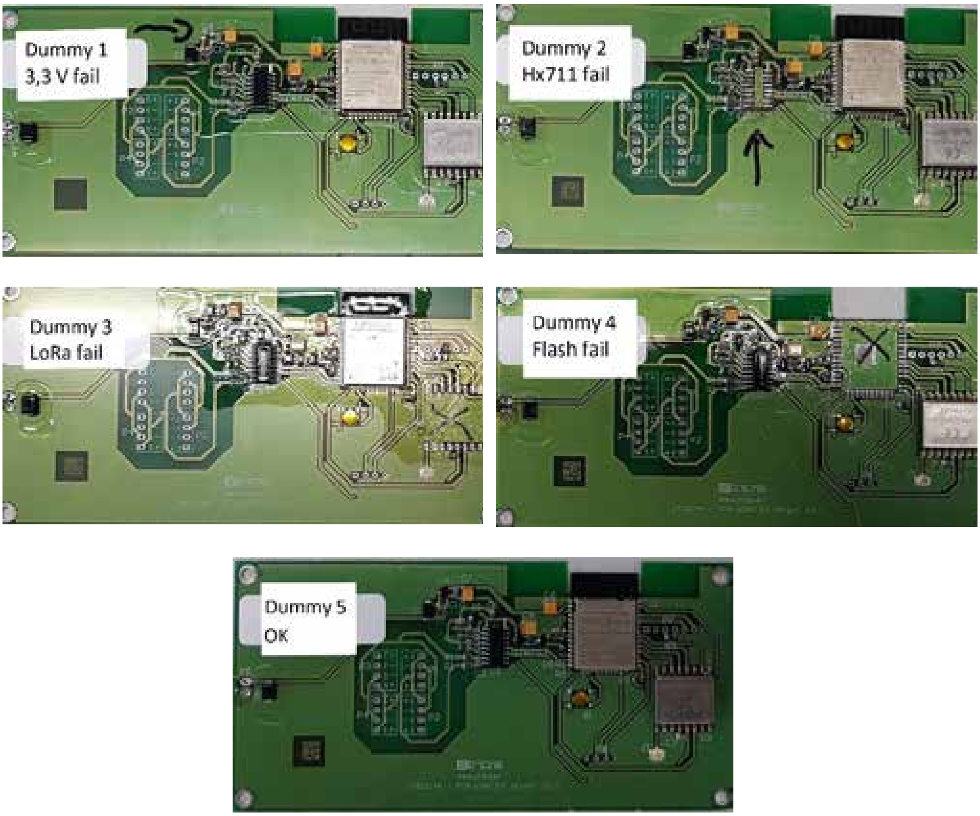

Figure 7: *PCBA functional tests*

The function test must be planned for both nests and cover all possible errors. Maintenance of the testing device is crucial because we need to ensure reliable operation for a long lifespan. The device must be maintained by lubricating the rods and the AMF clamp. The pushrods that push the tested PCBA in the nest need to be checked so they are not loosened, and the contact probes need to be inspected for any damage or dirt so there is no extra electrical resistance.

An analysis of a small series of 120 measurements was made on the second PCBA. The essential evaluation is the time of the measurement and the successful search for errors. In the series of 120 measurements, only three failures were detected, one defect of the 3.3 V linear voltage regulator and two failures on the LoRa module. The success of the measurements is shown in Figure 9.

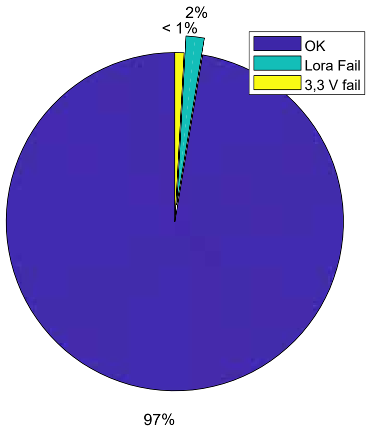

Figure 8: *Success of measurements*

The average time of the measurements without errors is 28.5 seconds. Most of the time is consumed when the testing and final program are uploaded. In case of failure, the time is shorter and depends on the error. The 3.3 V linear regulator measurements were analysed, and their results are presented in Table 1.

Table 1: *Statistical parameters of the 3.3 V linear regulator*

Parameter	Value
Maximal value	3.312205 V
Minimal value	3.278544 V
Average	3.293518 V
Median	3.292965 V
Variance	0.000030588
Standard deviation	0.00555526

The normal distribution of the 3.3 V linear regulator is shown in Figure 9, which displays minimal deviation, indicating positive results and quality of the measurement method with the ADC of the linear regulator.

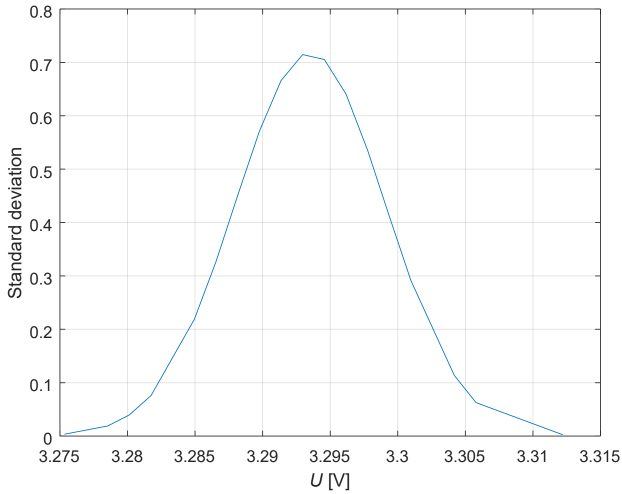

Figure 9: *Normal distribution of the 3.3 V linear regulator*

4 CONCLUSION

The intelligent measuring system, or the so-called testing device, ensures quality from the assembly line. Through the paper, an innovative method of designing a smart measurement system is presented, and therefore an advanced method for quality assurance of the product is realised. Electrical, mechanical and computer engineering knowledge is concentrated in a very complex product like the testing device. The housing protects the measurement equipment, allowing us to provide a safe work environment for workers. A reliable electrical connection with the tested PCBA is provided by the nest, which is one of the most crucial parts of the testing device. The electronics enable an intelligent measuring system that automates the measurements and speeds up the process in combination with programming. Successfully integrated testing devices are raising the quality of the products, lowering the proportion of defective devices being sold, and lowering the number of product returns. Testing devices are crucial in the PCBA industry and can be used for testing different products and materials. Unfortunately, the indestructible method is not always the most convenient technique to determine a product's functionality. However, it is desirable because it does not damage the product while testing its workflow. Intelligent measuring systems are also used in some maintenance programs and by some buyers in-house.

References

[1] **V. Anand, V. Singh and V. K. Ladwal:** „Study on PCB Designing Problems and their Solutions," 2019 International Conference on Power Electronics, Control and Automation (ICPECA), 2019, pp. 1-5.

[2] **M. Stan, N. Fidel, I. Mina and A. Husu:** „Improvement of Wireless Power Transfer Efficiency for Home Electronics and Appliances with the Use of SMD Components," 2018

10th International Conference on Electronics, Computers and Artificial Intelligence (ECAI), 2018, pp. 1-4.

[3] **M. Hirvikorpi**: "On the tactical level production planning in flexible manufacturing systems", ResearchGate, 2005**.**

[4] **V. Tsenev, V. Videkov and N. Spasova:** „Measurement of PCBA (Printed Circuit Board Assembly) Deformation During Functional Testing of Electronic Modules", 2021 International Conference on Information Technologies (InfoTech), 2021, pp. 1-5.

[5] **P. Kosky, R. Balmer, W. Keat, G. Wise:** "Exploring Engineering (Third Edition)", Chapter 9–Electrical Engineering, Academic Press, 2013, pp. 185-203.

[6] **B. Haraoubia:** „ 2–Analog-to-Digital and Digital-to-Analog Converters „, 2019, Non-Linear Electronics 2, Elsevier, pp. 99-190.

[7] **B. A. Gregory:** „Electrical and Electronic Measurement", 2003, Encyclopaedia of Physical Science and Technology (Third Edition), pp. 1-37.

[8] **O. Mohammed, A. A. Rachida, D. Olivier, M. Abdelaziz:** „An open source and low-cost Smart Auditorium", 2021, Procedia Computer Science, (Volume 191), pp. 512-523.

[9] **Feinmetall**. Available online: https://www.feinmetall.com/products/contact-probes/ (accessed on 27 October 2022).

Journal of Energy Technology

Author instructions

www.fe.um.si/jet.html

MAIN TITLE OF THE PAPER
SLOVENIAN TITLE

Author[1], Author [2], Corresponding author[ℜ]

Keywords: (Up to 10 keywords)

Abstract

Abstract should be up to 500 words long, with no pictures, photos, equations, tables, only text.

Povzetek

(Abstract in Slovenian language)

Submission of Manuscripts: All manuscripts must be submitted in English by e-mail to the editorial office at jet@um.si to ensure fast processing. Instructions for authors are also available online at http://www.fe.um.si/en/jet/author-instructions.html.

Preparation of manuscripts: Manuscripts must be typed in English in prescribed journal form (MS Word editor). A MS Word template is available at the Journal Home page.

A title page consists of the main title in the English and Slovenian language; the author(s) name(s) as well as the address, affiliation, E-mail address, telephone and fax numbers of author(s). Corresponding author must be indicated.

Main title: should be centred and written with capital letters (ARIAL bold 18 pt), in first paragraph in English language, in second paragraph in Slovenian language.

Key words: A list of 3 up to 6 key words is essential for indexing purposes. (CALIBRI 10pt)

Abstract: Abstract should be up to 500 words long, with no pictures, photos, equations, tables, - text only.

Povzetek: - Abstract in Slovenian language.

Main text should be structured logically in chapters, sections and sub-sections. Type of letters is Calibri, 10pt, full justified.

ℜ Corresponding author: Title, Name and Surname, Organisation, Department, Address, Tel.: +XXX x xxx xxx, E-mail address: x.x@xxx.xx

[1] Organisation, Department, Address

[2] Organisation, Department, Address

Units and abbreviations: Required are SI units. Abbreviations must be given in text when first mentioned.

Proofreading: The proof will be send by e-mail to the corresponding author in MS Word's Track changes function. Corresponding author is required to make their proof corrections with accepting or rejecting the tracked changes in document and answer all open comments of proof reader. The corresponding author is responsible to introduce corrections of data in the paper. The Editors are not responsible for damage or loss of submitted text. Contributors are advised to keep copies of their texts, illustrations and all other materials.

The statements, opinions and data contained in this publication are solely those of the individual authors and not of the publisher and the Editors. Neither the publisher nor the Editors can accept any legal responsibility for errors that could appear during the process.

Copyright: Submissions of a publication article implies transfer of the copyright from the author(s) to the publisher upon acceptance of the paper. Accepted papers become the permanent property of "Journal of Energy Technology". All articles published in this journal are protected by copyright, which covers the exclusive rights to reproduce and distribute the article as well as all translation rights. No material can be published without written permission of the publisher.

Chapter examples:

1 MAIN CHAPTER

(Arial bold, 12pt, after paragraph 6pt space)

1.1 Section

(Arial bold, 11pt, after paragraph 6pt space)

1.1.1 Sub-section

(Arial bold, 10pt, after paragraph 6pt space)

Example of Equation (lined 2 cm from left margin, equation number in normal brackets (section. equation number), lined right margin, paragraph space 6pt before in after line):

Equation (1.1)

Tables should have a legend that includes the title of the table at the top of the table. Each table should be cited in the text.

Table legend example:

Table 1: *Name of the table (centred, on top of the table)*

Figures and images should be labelled sequentially numbered (Arabic numbers) and cited in the text – Fig.1 or Figure 1. The legend should be below the image, picture, photo or drawing.

Figure legend example:

Figure 1: *Name of the figure (centred, on bottom of figure, photo, or drawing)*

References

[1] **N. Surname:** *Title,* Journal Title, Vol., Iss., p.p., Year of Publication

[2] **N. Surname:** *Title,* Publisher, Year of Publication

[3] **N. Surname:** *Title* [online], Publisher or Journal Title, Vol., Iss., p.p., Year of Publication. Available: website (date accessed)

Examples:

[1] **J. Usenik**: *Mathematical model of the power supply system control*, Journal of Energy Technology, Vol. 2, Iss. 3, p.p. 29 – 46, 2009

[2] **J. J. DiStefano, A.R. Stubberud, I. J. Williams**: *Theory and Problems of Feedback and Control Systems*, McGraw-Hill Book Company, 1987

[3] **T. Žagar, L. Kegel:** *Preparation of National programme for SF and RW management taking into account the possible future evolution of ERDO* [online], Journal of Energy Technology, Vol. 9, Iss. 1, p.p. 39 – 50, 2016. Available: http://www.fe.um.si/images/jet /Volume 9_Issue1/03-JET_marec_2016-PREPARATION_OF_NATIONAL.pdf (7. 10. 2016)

Example of reference-1 citation: In text *[1],* text continue.

Nomenclature

(Symbols)	(Symbol meaning)
t	time

JET I Journal of Energy Technology I Vol. 15, Issue 3, November 2022 I University of Maribor, Faculty of Energy Technology

ISSN 1855-5748

9 771855 574008